6

From Nanosize Silica Spheres to Three-Dimensional Colloidal Crystals

Siegmund Greulich-Weber and Heinrich Marsmann
Department of Physics, Faculty of Science, University of Paderborn, D-33095 Paderborn, Germany
greulich-weber@physik.upb.de

6.1. INTRODUCTION

Nanometre-scale periodic porous structures exhibit many unique optical, electrical and mechanical properties that can be exploited in a wide range of applications from photonics and electronics to biological and medical sensing. The synthesis of sub-micrometre building particles and their assemblies, such as silica or polystyrene spheres [1–8], nanotubes [9–15], nanowires [16–22] and nanocrystals [23–26], are of significant importance for the development of advanced nanotechnology. It is worthwhile to notice that there still remains a great challenge in synthesizing nanoporous materials with highly and precisely controlled pore sizes in ordered three-dimensional structures in large volumes [27–31]. A promising technique for fabricating 3D nanoporous structures is based on the self-assembling growth of monodisperse spherical colloidal particles of silica or polystyrene, further on called nanospheres. From such three-dimensional periodical packages, so-called colloidal crystals or opals, useful nanostructured materials can be created by replicating these crystals in a durable matrix that preserves their key feature of a long-range periodic structure. The fidelity of this procedure is mainly determined by the crystal growth mechanisms of opals and the monodisperity of nanospheres. Therefore in Section 6.2 methods for obtaining and modifying monodisperse silica spheres are reviewed [32–35], which mainly rely on the process invented by Stoeber [6]. Latex spheres are usually obtained by emulsion polymerization, which was described in detail elsewhere [36–42]. In Section 6.3 important mechanisms for growing opals from

nanospheres are discussed. Since the dense packing (fcc, hcp) of monodisperse spheres creates regular voids, these crystals already belong to the family of nanoporous materials. By using colloidal crystals as templates inverted structures can be created by filling the voids with other materials and afterwards releasing the nanospheres. The porous materials obtained by this approach have also been referred to as "inverted opals" or "inverse opals" because they have an open, periodic 3D framework complementary to that of an opal structure. Their fabrication, properties and applications are discussed in Section 6.4. Finally, in Section 6.5 a by far not complete review of actual and promising applications is given.

6.2. SYNTHESIS OF COLLOIDAL SILICA NANOSPHERES

Many compounds of the 6th group of the periodic table of the elements such as oxides, sulphides, etc. are insoluble in aqueous solutions. This behaviour can be used to generate small particles by chemical reactions. The properties of a number of metal oxide particles have been described in [1–3,43]. Depending on their crystallinity, spheres, cubes or needles of several nanometres diameter are observed. Because of quantum size effects the small particles build up have different properties compared to bulk material. If they are small enough they stay in solution forming sols. Prominent metal colloids are build, e.g., from gold, which displays red colour. Spheres of diameters up to several hundred nanometres are grown from silicon dioxide. The synthesis and properties of these amorphous silica spheres are the topic of large number of review articles [4,5]. Especially the observation made by Stoeber *et al.* [6] that silica spheres can be grown almost perfectly as monodisperse colloidal spheres has fascinated meanwhile generations of researchers. The synthesis and modification of these nanometre-sized silica spheres will be discussed in the following.

6.2.1. Synthesis

Generally the formation of silica is a two-step process starting from a source of silicic acid and followed by a condensation resulting in an amorphous gel particle. This condensation process leads to individual particles or a gel spanning the whole container. Most of the syntheses start from an organic ester of the silicic acid, e.g., tetraethoxisilane, $(C_2H_5O)_4Si$, usually abbreviated to TEOS. The first step is the hydrolysis, which is followed by the condensation over the silanol groups:

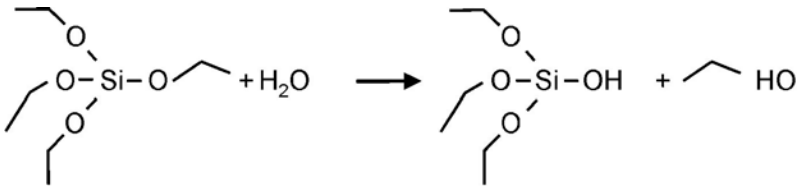

(6.1)

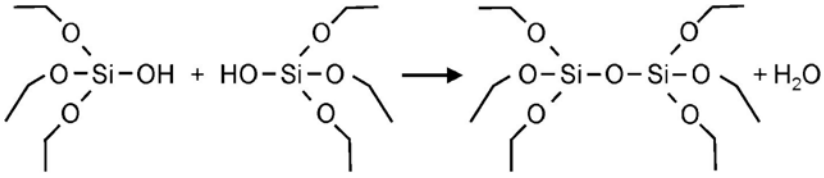

(6.2)

Because TEOS has four ethoxy groups three- and fourfold reactions lead to 3D networks. Both reactions are moderated by a catalyst, usually ammonia, NH_3, as in the original Stoeber approach [6] or acetic acid as used in [7] or hydrochloric acid as described in [44]. Further sources suitable as silicic acid are feasible, e.g., aqueous solutions of water glass, or other esters of silicic acid, e.g., tetramethoxisilane, $(CH_3O)_4$, TMOS (because of its highly poisonous nature the use of TMOS is not encouraged). The overall reaction can be dissected into two parts. The first is the initiation step where the primary particles are formed which is followed by the growth of the particles as long as silicic acid is available.

The formation of monodisperse, uniform and smooth spheres in the Stoeber process has attracted much interest. The reactions take place in a mixture of water and a lower alcohol such as ethanol with a varying amount of ammonia. Depending on the concentration of the components of the reaction and the reaction temperature spheres with diameters between 50 and 2000 nm have been synthesized. It was observed that the smallest particles grow best in methanol, while the largest in butanol. An increase of the concentration of ammonia caused larger diameters of the spheres, while the amount of water was of minor influence [6].

Basically there are two theories explaining the particle growth. One involves the accumulation of monomeric or small condensates of silicic acid to form primary particles. It is assumed that during growth no further primary particles are formed and that the growth of the particles occurs by aggregation of monomers [45–48]. The particle growth is reaction limited and depends on the reaction rate of the hydrolysis of the silicic acid ester.

According to an alternative theory, there is a continuous generation of primary particles which merge with larger particles causing their further growth [49,50]. A study of the particle growth by cryogenic transmission electron microscopy clearly shows that small, low-density particles coalesce forming primary particles. However, in the following, no evidence of smaller, dense particles besides the large growing spheres was observed [51]. Possible formation of irregular-shaped particles was claimed to be the result of an aggregation of larger particles [48]. The simultaneous growth of silica particles of different sizes is possible if the concentration of the alkoxide is kept low. If no new particles are generated, all particles grow with the same rate pointing to a surface-limited reaction. If the concentration of TEOS is high enough allowing the generation of new particles, the smaller particles will grow faster than the larger ones, thus indicating that their growth is diffusion limited [52]. A mathematical model describing the generation of monodisperse spheres explains the monodisperity as a function of the interfacial energy of the solution–particulate system without the need of a separate nucleation phase [53].

A precise control of the number of primary particles during the nucleation phase is difficult. Therefore the size of particles synthesized under identical conditions varies by about 20% in each batch, although they are still monodisperse. The most successful procedure of obtaining a certain size of spheres is to start from a solution of spheres smaller than intended and use them as a seed. The gradual addition of TEOS using Stoeber conditions lets the spheres grow to the desired size [48,55].

Besides the usual procedure synthesizing silica particles by hydrolysis or condensation in alcohol water mixtures, silica spheres may also be grown in micelles. The reaction medium consists of water and, e.g., an ionic surfactant such as benzethonium chloride [56], a non-ionic one such as nonyl phenol ethylene oxide [46,57] or a block copolymer and several alcohols [58]. The advantage of such a procedure is the possibility of obtaining nanospheres of difficult monomers, e.g., a mixture of TEOS and methyltrimethoxysilane. The size of the particles is determined by the ratio of surfactant to monomer [46,56,57] or the flexibility of the organic part of the alcohol [58]. It seems that very small particles can be obtained with the help of micelles. Diameter of about 10 nm has been reported [56]. It is remarkable that cetyltrimethylammonium bromide as a surfactant yields with TEOS and water irregular mesoporous silica spheres with highly ordered pores while adding ethanol to the reaction mixture gave smooth spheres with starburst pores [59]. Silica spheres with zeolite-type mesopores are also synthesized with the help of surfactants [60,61].

^{29}Si magic angle nuclear magnetic resonance (MAS-NMR) affords insight into the microstucture of the silica spheres. Because of the fact that silicon connected by four siloxane bonds to other silicon atoms (Q^4 groups) has a chemical shift (~ -110 ppm) different to silicon connected to three (Q^3 groups, ~ -100 ppm) or two silicon atoms (Q^2 groups, ~ -90 ppm). It was observed that the silica prepared according the Stoeber process contains about two thirds of Q^4 groups and one third of Q^3 groups and only a few per cent of Q^2 groups. Silica obtained with the help of nonyl phenol ethylene oxide has a more open structure, due to the higher content of Q^3 groups. The open valences of $Q^3$and Q^2 groups are saturated by ethoxy residues confirmed by ^{13}C MAS-NMR [4].

6.2.2. Modification of Silica Spheres

As interactions between silica spheres are required to tune their physical properties according to the needs of intended applications, it is necessary to design their chemical composition. Furthermore, the spheres have to be dried for almost all applications, which might change their properties drastically. The structure, size and composition of these hybrid particles can be altered in a controllable way to tailor their optical, electrical, thermal, mechanical, electro-optical, magnetic and catalytic properties over a broad range. In the following several ways to achieve appropriate requirements are pointed out.

6.2.2.1. Modification with Organic Residues. The motivation to modify silica particles with organic residue is mainly due to the following reasons.

The reaction between two silanol groups (Equations (6.1) and (6.2)) might also happen when two silica particles touch each other. This leads to irreversible connections between the particles and will prevent resuspension in a solvent. By modifying the surface

with organic groups the surface of the particles will be protected and the particles may receive new properties suitable for the surrounding solvent.

An organic modification might be realized in order to obtain new functionalities, e.g., for bonding with polymers or with chromophores.

One simple example is the surface modification of silica spheres with stearyl alcohol, a long-chain alcohol [62,63]. Also octadecanol was used to form a protective shell around the silica particles [60], and methods were used to attach polystyrene chains via silanol groups [64] or polyisobutene [65]. In that way silica particles were made more compatible to organic solvents and their surfaces deactivated. More versatile are procedures of introducing organic functional groups. Rather easy to synthesize and commercially available are trialkoxyorganosilanes, where alkoxy groups can react with the silanol groups of silica, forming surface modified silica. Alternatively they might be mixed with the TEOS reacting to a copolymer. The organic chain mostly a propyl residue carries a functional group R1 such as a halogen, an ammino or a mercapto group.

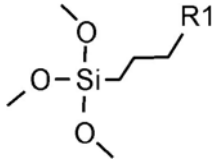

(6.3)

The modifiers and examples given above or in the literature are tabulated in Table 6.1. Functional groups have been used to attach dyes such as fluorescein [60,66,67] or rhodamine [60] or to form a network in epoxy composite material [68]. It was suggested that the dye molecules (fluorescein) tend to form clusters during the synthesis of the colloidal spheres [66]. Reactions with trimethoxysilylated polymers such as poly(maleic anhydride-costyrene) or poly(methacrylate) lead to silica spheres with a coat of polymer.

There are interesting proposals to incorporate inorganic ions and compounds in the silica to make use of their optical properties. CuO was infiltrated in MCM-41-type silica nanospheres in a Stoeber-type synthesis of silica particles [61]. The chemical degradation of alkyldithiocarbamato complexes of cadmium in the presence of sub-micrometric SiO_2 particles results in the formation of CdS nanoparticles on the sphere surface [69]. Because most metal ions form precipitates in basic solution, the synthesis of silica particles under acidic catalysis is of advantage. The incorporation of rare earth ions in silica spheres is interesting for photonic purposes succeeded in that way. Pr^{3+} and Eu^{3+} could be found in silica spheres, when TEOS was reacted in a mixture of water and acetic acid. The

TABLE 6.1. Selected organic modifiers for silica.

Reagent	Reference
$NH_2(CH_2)_3Si(OC_2H_5)_3$	[28,29,30,33,34]
$NH_2(CH_2)_3Si(CH_3)(OC_2H_5)_2$	[32]
$HS(CH_2)_3Si(OC_2H_5)_3$	[28]
$ClC_6H_4Si(OCH_3)_3$	[31]
$CH_3C_6H_3(NCO)_2$	[32]
Epichlorhydrin	[32]

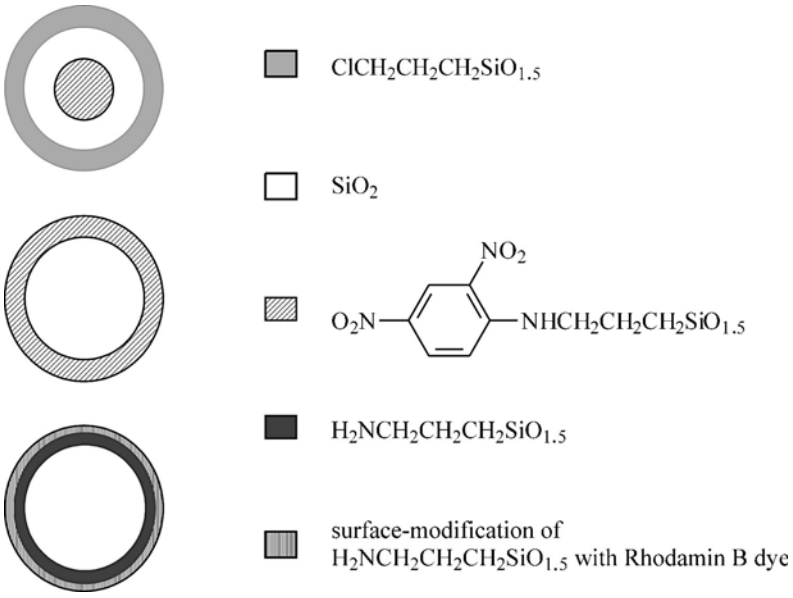

FIGURE 6.1. Schematic representations of different core-shell designs for silica spheres. Details are given in the text and in Table 6.2.

particles exhibited bright room-temperature luminescences when excited by an argon ion laser at 488 nm [70]. Er^{3+} and Tb^{3+} ions could be incorporated by an analogous procedure [71], while silver nanoparticles (∼2–5 nm) inside silica spheres could be generated by photochemical reduction of silver nitrate [72].

6.2.2.2. Core-Shell Designs. The growth of silica spheres by a slow generation of silicic acid by, e.g., hydrolysis of TEOS could be used to form additional layers on them. Several design models are possible. An example is given in Figure 6.1. Several examples are possible and worked out. The interested reader is referred to the literature [73]. A recent review on nanoengineering of spherical particle surfaces was, e.g., given by Caruso [74]. Further special designs for various applications are given in [28,54,75–79]. A collection of selected layer structures is summarized in Table 6.2. Some interesting materials for photonic applications could be made this way. Especially promising seems the inclusion of highly refractive compounds such as metals, oxides and sulphides.

The core-shell design is a clever tool to modify the properties of the particles. For instance, a chromophore can be put on the shell to interact with chemical influences from outside while by placing the same modifier inside it will shield against the environment. It is possible to tailor a composite particle in which every layer will confer a special property to it [33,38].

6.2.2.3. Infiltration and Doping. Besides the core-shell method, which allows a modification of silica spheres during the sphere synthesis, other materials such as semiconductor nanocrystallites, metal sols and organic chromophores have been incorporated

TABLE 6.2. Examples of core-shell silica particles.

Core	1th layer	2nd layer	Reference
SiO_2 + APS[a]	SiO_2		[30]
SiO_2 + APS + Dye	SiO_2		[33]
SiO_2	SiO_2 + APS + Dye		[33,38]
SiO_2	SiO_2 + APS + Dye	SiO_2 + octadecanol	[33,38]
SiO_2	Ag		[21]
$\alpha-Fe_2O_3$	SiO_2		[43]
ZnS	SiO_2		[44]
SiO_2	ZnS		[44,45]
SiO_2	SiO_2 + CdS	SiO_2	[39]

[a]3-Aminopropyltriethoxysilane.

into silica colloids during the synthetic step in order to functionalize these particles with useful optical, electrical or magnetic properties [75–77]. However, the distribution of the materials incorporated is less homogeneous in comparison to the core-shell method.

Another way of modifying nanospheres usually used for catalytic applications is to infiltrate them with suitable materials after their synthesis [80–87]. This can be done by either adding salts to the solvent containing the material intended to deposit in the porous nanospheres or by allowing a chemical reaction of cations with the inner surface of the spheres or the residual organic content left from the sphere synthesis. The latter is present even after careful cleaning of the spheres after their synthesis. However, if the desired material is incorporated into the sphere's silica matrix, one may call this doping of silica. Most probably this will not happen at room temperature. Heating the material will allow the doping ions to further diffuse into the porous silica (see the next section). Such a kind of doping is considerably more stable than "fixing" the infiltrated material at some residual organic content which might partly evaporated during drying the spheres even at room temperature.

With the further on so-called galvanic method electric-field-driven ions in the solvent are captured by the porous spheres between two electrodes [88,89]. The galvanic method works most efficiently for metal ions and allows an effective infiltration at room temperature allowing afterwards the same chemical reactions as described above or additional temperature treatments.

There are a few more expensive methods to modify the properties of silica spheres such as, e.g., ion implantation [90–93]. Another less expensive method that finally should be mentioned is infiltration of dried spheres in a dopant gas phase, which of course is most effective at high temperatures [87].

6.2.2.4. Thermal Treatment. The spheres in an opal structure as discussed in Section 6.3 are held together just by relatively weak forces. For applications cracking or disrupting the structure is always a problem. By sintering, annealing or heating silica spheres above the glass point it is possible to strengthen the material. Pristine samples of silica colloids will undergo a series of changes when they are thermally treated at elevated temperatures. First the absorbed water will be released at $\sim$150 °C. In the temperature range of 400–700 °C the silanol groups will be crosslinked via dehydration. Finally,

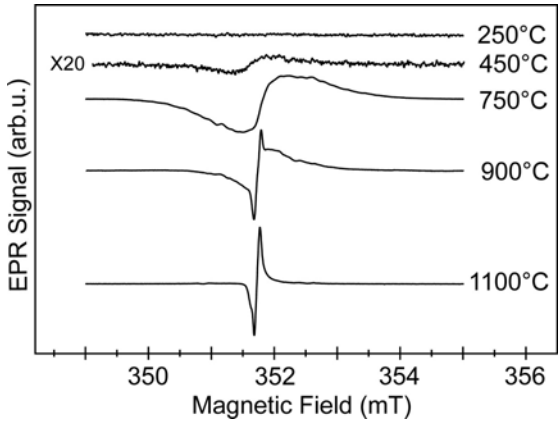

FIGURE 6.2. EPR spectra of undoped silica spheres (1200 nm diameter) measured at $T = 10$ K and a microwave frequency of 9.42 GHz [87]. As grown silica spheres do not show an EPR spectrum (upper trace). After annealing at different temperatures for 1 hour each new EPR spectra appear, which are discussed in detail in the text.

these particles will start to fuse into aggregates when the temperature is raised above the glass transition temperature of amorphous silica (∼800 °C). These steps are clearly observable with suitable spectroscopic methods. Electron paramagnetic resonance (EPR) turned out to be a particularly helpful tool, showing all steps as presented in Figure 6.2 [87]. While after drying the spheres no EPR was observed, around 400 °C an EPR signal appeared, which again decreased at the expense of a completely different signal which became strongest above 1000 °C. The broad and asymmetric signal observed at around 750 °C (Figure 6.2) is a typical signal of an amorphous surface defect in the porous silica matrix [87]. The EPR spectrum shown for annealing at 1100 °C (see Figure 6.2) has a comparably small line width and is symmetric with respect to the baseline, being more typical for a crystalline or polycrystalline environment. Further small satellite lines, not shown in Figure 6.2, are due to the interaction of an unpaired electron with two different ^{29}Si neighbours. A similar spectrum is known from the so-called E′ centre in SiO_2 [94], a dangling bond centre at the SiO_2 surface. Figure 6.2 implies that the EPR may serve as a tool for controlling the heat treatment of silica spheres, which is unavoidable for the realization of nanoporous materials discussed in the next sections.

The transition from a less dense amorphous gel composition to a glass-like structure is also seen in the optical transmission spectra, showing that the spheres became more transparent in the visible range after annealing at 1000 °C (Figure 6.3) [87].

Finally the transition from the dried gel state to the glass-like state results in a further decrease in sphere diameter (∼5%), which was demonstrated by electron microscopy as shown in Figure 6.4 [87].

Spectroscopic control becomes even more important in the case of sphere infiltration or doping. As an example Figure 6.5 shows EPR spectra of Cu-infiltrated silica spheres. The lower trace in Figure 6.5 is observed without heat treatment either after Cu-infiltration using copper chloride, copper sulphate or copper nitrate as solvents or after infiltration by the galvanic method [87]. The latter turned out to be the most efficient one. The EPR

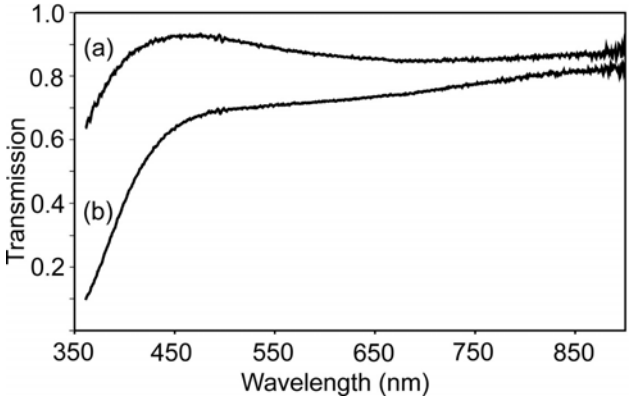

FIGURE 6.3. Transmission spectra of undoped dried silica spheres (400 nm diameter) otherwise as grown (a) and after annealing for 1 hour at 1000 °C (b) [87].

spectrum (Figure 6.5, lower trace) belongs to a Cu^{2+} complex containing nitrogen [95] in an amorphous environment (strictly speaking hexamine copper nitride). Independent of the infiltration process used the EPR spectrum completely vanished after heat treatment at about 1000 °C. Along with that the colour of the silica spheres changed from light blue to dark red. A similar change in colour is observed if untreated spheres are electron-irradiated; however, in that case a new EPR spectrum is observed probably due to an intrinsic defect [87].

Though we end up with the same colour, obvious different reasons accidentally lead to the same colour. Optical spectroscopy helps showing different transmission spectra. As

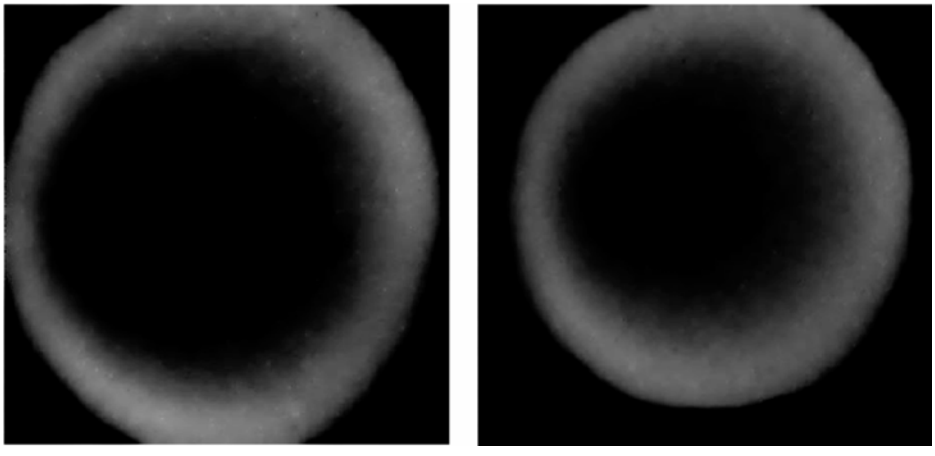

FIGURE 6.4. Transmission electron microscopy (TEM) images of single spheres which as grown had a diameter of 1.2 μm (as determined by dynamical light scattering, Huber). The left image shows a sphere after drying. The total size of the image is $1 \times 1 \mu m^2$. The right image shows one sphere from the same batch of silica spheres but after heat treatment at 1000 °C for 1 hour [87].

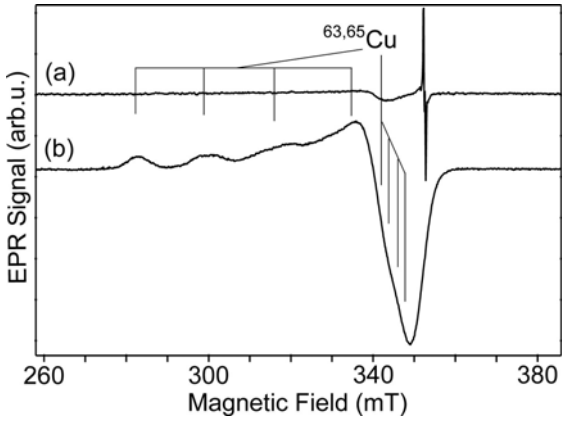

FIGURE 6.5. EPR spectra of Cu-infiltrated silica spheres (for details see the text), measured at T = 10 K and a microwave frequency of 9.42 GHz. As grown and afterwards dried independent of the fabrication procedure a Cu-related EPR spectrum is observed (lower trace). After heat treatment at T > 400 °C a new EPR spectrum appears. Without annealing, but with electron irradiation the same EPR spectrum is observed. Details are discussed in the text. Further information on the parameters describing the EPR is given in [87].

an example Figure 6.6 presents the spectrum obtained after Cu-infiltration and a following heat treatment, showing a plasmon resonance at around 600 nm. This indicates that the Cu^{2+} EPR signal vanished because metal colloids are built due to the heat treatment [87]. The red colour appearing after electron irradiation is a result of an indirect charge transfer effect.

Cu-infiltrated silica spheres illustrate the need to control the modification of spheres by adequate methods. The most helpful tool for controlling the actual realization of sphere modifications is EPR resolving the microscopic and electronic structure of the dopants and their local environment with high sensitivity. Complementary optical investigations

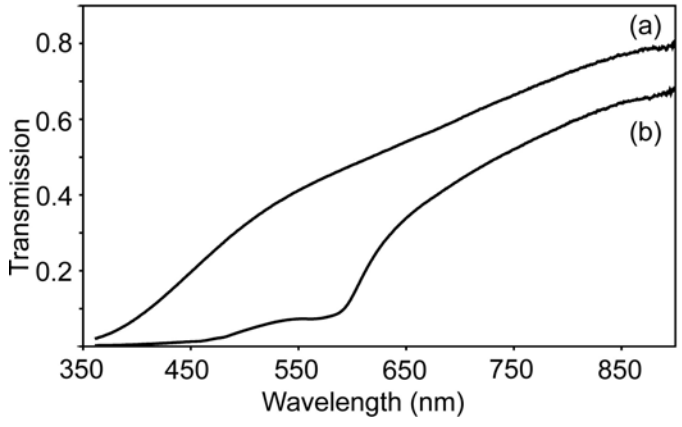

FIGURE 6.6. Transmission spectra of Cu-doped and dried silica spheres (400 nm diameter) (a) and after annealing for 1 hour at 1000 °C (b) [87].

are indispensable. Furthermore, geometrical variations are best observed via electron microscopy; under best conditions also details of the dopant distribution are observed.

So far using preparation methods as described above several materials have been successfully incorporated into silica spheres for different applications. Besides the use for medical [95–97] or catalytic applications [61,98] there are promising developments based on magnetic particles [99–104] or metal ions [99,101,104–108]. For most applications aggregated spheres, often periodically arranged, are needed instead of single spheres. Thus capabilities to fabricate ordered structures of spherical colloids are discussed in the following section.

6.3. GROWTH OF COLLOIDAL CRYSTALS

In nature silica spheres sometimes crystallize into colloidal crystals of fcc structure through self-assembly known as opals. In the following we describe procedures for growing artificial opals [109–113] and so-called inverted opals [27,114–124], which are negative replica of opal structures. In principle, there are three common techniques for obtaining artificial opals from monodisperse silica nanospheres stored in protic solvents. Since the density of SiO_2 is significantly larger than that of water (or related hydrogen solvents) sedimentation is the dominating method for growing bulk crystals [125]. On the other hand, the silica spheres experience attractive capillary forces at the solvent surface due to evaporation of the solvent, leading to self-assembly of spheres close to the surface. This method is commonly used for growing thin film opals. Both methods critically depend on competing interactions between spheres themselves and between spheres and environment. Another attempt is to ignore these interactions by applying strong external forces such as centrifugation [118,126,127] or electrophoresis [128–130]. However, in this case no self-assembly of the spheres is expected and additional agitation is needed to improve crystalline quality.

Opal growth by self-organization of monodisperse silica spheres is of course the most interesting and by far most intensive studied phenomenon. Charged silica colloids suspended in a protic solvent interact through hard-core repulsions, van der Waals attractions, Coulomb interactions and hydrodynamic coupling. The influence of the spheres on the surrounding medium modifies these interactions, for instance leading to screening of Coulomb interactions or giving rise to entropically driven depletion interactions in heterogeneous suspensions. Solvents usually used are, e.g., water or ethanol.

In the following relevant interactions responsible for growth mechanisms of colloidal crystals from a diluted suspension of monodisperse silica spheres will be represented briefly.

6.3.1. Interactions Between Colloidal Particles

6.3.1.1. Coulomb Interaction. The acidity of the silanol groups causes a negative charge of the silica particles [5]. The isoelectric point of the particles can be altered by surface modification, e.g., for a pH value of about 3 for amino group functionalized particles [4]. Therefore silica spheres always carry surface charges due to adsorbed ions or electrons, and due to the dissociation of polar groups at the surface the Coulomb

interaction is the most important. Furthermore, the solvent itself contains moveable charges (dissolved salts). Unaffected by the kind of charges dissolved ions are mainly found at the complementary charged silica spheres. A shell of ions is precipitated, the so-called Stern layer [131]. The strength of this Coulomb energy dissipates exponentially away from the surface as the concentration of further ions of this layer follows Boltzmann's law. Using this space charge distribution the resulting potential can be derived by the Poisson equation. The mathematics that describes the electrostatic force finds its origin in the Poisson–Boltzmann distribution [132]:

$$\nabla^2 \phi(r) = \kappa^2 \phi(r). \tag{6.4}$$

Numerous models have been developed from this fundamental relationship. Simplified models are based on assumptions about particle geometry, surface charge and potential [133]. An electrostatic interaction energy model used to describe the commonly encountered geometry of a sphere and a flat plate in water is, for example, given by Gregory [134] (see also [133]).

Solving the Poisson–Boltzmann equation for the long-range Coulomb repulsion shielded by electrolytes outside a sphere of radius R carrying charge $z_1 e$ yields a Yukawa potential [135]:

$$\phi(r) = \frac{z_1 e}{4\pi\varepsilon(1+\kappa R)} \frac{\exp[-\kappa(r-R)]}{r}. \tag{6.5}$$

The potential is repulsive and steep compared to the sphere radius. The particle charge can be determined easily from the mobility in an electric field and is about $10^{-16}\,\mathrm{C} = 10^3 \mathrm{e}^-$. The remaining ions in an otherwise ion-poor solvent do not influence the estimation made above [136].

κ in Equations (6.4) and (6.5) is the reciprocal Debye–Hückel length of the solvent [137]

$$\kappa^2 = \frac{e^2}{\varepsilon k_\mathrm{B} T} \sum_{i=2}^{\infty} n_i z_i^2 \tag{6.6}$$

with z_i the valence and n_i the concentration of ion i. An increase in electrolyte concentration results in a decrease in the Debye–Hückel length and concomitant reduction in the electrostatic interaction energy due to the shielding effect of the ion shell of the sphere on the Coulomb potential. At a specific salt concentration, known as the critical coagulation concentration, the electrostatic interaction force can be virtually neutralized. Changes in pH influence the range and magnitude of electrostatic forces. Reactions between protons and charged surface functional groups can change the net surface potential on a particle [138].

6.3.1.2. Van der Waals Attraction. The van der Waals attraction is a common interaction of all matter. In the case of silica spheres one has to integrate over all dipoles of spheres, which can be done easily because of the simple geometrical properties of a pair of spheres. The interaction energy results in the following attractive potential [139],

$$\phi(r) = -A_{12} \frac{R}{12r} \tag{6.7}$$

with the sphere radius R, the distance r between two spheres and the constant A_{ij} for the material combination. A_{ij} is known as the Hamaker constant [140,141] and is proportional to the square of the polarization of a material. In the theory of Hamaker the constant A is given as the sum of A_{ij} over single terms of the combination of two materials (ij) which are tabled [142]. For two particles consisting of materials 1 and 2, respectively, in a solvent (medium 3) the Hamaker constant is calculated by [132,143]

$$A_{123} = A_{12} + A_{33} - A_{13} - A_3. \tag{6.8}$$

So far the competing electrostatic interactions, the screened Coulomb and the attractive van der Waals interaction (now expanded including dispersion effects) have been discussed as the main interactions between charged objects in an electrolyte. However, further interactions have to be considered (see below) while it was recently argued that both electrostatic interactions discussed so far cannot be considered separately [144–146].

Attempts to quantitatively describe colloidal interactions [147,148] resulted in the famous DLVO (Derjaguin–Landau–Verwey–Overbeek) model. The DLVO theory was developed by balancing attractive dispersion (London, van der Waals) and repulsive electrostatic Coulombic forces and meanwhile had been accepted to be inclusive of all primary interfacial forces of significance. Both van der Waals and Coulombic forces can be either repulsive or attractive depending on chemical structure, suspending medium properties and surface potential.

6.3.1.3. DLVO Theory. The nonlinear Poisson–Boltzmann equation (6.4) has only been solved analytically for a very restricted set of geometries, parallel charged plates, for example [133,134]. Solutions for more general geometries such as pairs of spheres have proved elusive. Even this intractable model involves a dramatic simplifying approximation. The suspending fluid appears in Equations (6.4) and (6.5) only through its dielectric constant. This so-called primitive model completely neglects effects due to the structure of the solvent, an approximation which fails when the separation between nanospheres becomes comparable to a few molecular radii.

Derjaguin, Landau, Verwey and Overbeek (DLVO) [147,148] pushed the field forward in the 1940s by applying approximations from the Debye–Hückel theory of electrolyte structure [137,139].

The DLVO theory provides approximate solutions to the Poisson–Boltzmann equation describing the nonlinear coupling between the electrostatic potential and the distribution of ions in a colloidal suspension. It predicts that the effective pair interaction in dense suspensions sometimes has a long-ranged attractive component. The resulting interaction between isolated pairs of well-separated spheres has the form [149]

$$\frac{\phi(r)}{k_\mathrm{B}T} = Z_1^* Z_2^* \frac{e^{\kappa a1}}{1+\kappa a_1}\frac{e^{\kappa a2}}{1+\kappa a_2}\lambda_\mathrm{B}\frac{e^{-\kappa r}}{r} + \frac{V(r)}{k_\mathrm{B}T} \tag{6.9}$$

where r is the centre-to-centre separation between two spheres of radii a_i with effective surface charges Z_i^* in an electrolyte of the Debye–Hückel screening length κ^{-1}. $\lambda_B = e^2/k_\mathrm{B}T$ is the Bjerrum length, equal to 0.714 nm in water at $T = 24\,^\circ$C, and $V(r)$ is the Coulomb potential.

The full DLVO potential includes a term accounting for dispersion interactions (see above, extended van der Waals interaction), which, however, is negligibly weak for well-separated spheres [150,151].

6.3.1.4. Depletion Potential. Besides optimizing the above-described interactions between colloidal particles themselves and the solvent, further procedures are necessary for the growth of extended colloidal crystals of high quality. It was shown by Asakura and Oosawa [152] and independently recovered and further elaborated by Vrij [153] that the addition of a non-adsorbing polymer to a dispersion of colloidal particles will lead to an effective attractive interaction. The attractive interaction, which is called the depletion interaction, is the origin of a rich phase behaviour displayed by colloid–polymer mixtures. Depletion interactions can occur in systems that have particles with disparate sizes: for example, a system that contains large spheres in dispersion comprised relatively small colloids. As the large spheres approach one another, the smaller colloids will be excluded from the gap between them, which results in a decrease in osmotic pressure between the spheres. This reduction in osmotic pressure results in an attractive force called the depletion attraction. In Figure 6.7 this situation is sketched schematically.

The depletion interaction can be explained in terms of purely repulsive interactions between the polymers and the much larger colloidal particles. Each colloidal particle is surrounded by a shell with a thickness of the order of the radius of gyration of a polymer molecule through which the centre of the polymer cannot penetrate. This excluded region is called the depletion zone (see Figure 6.7a). When two colloidal particles approach each other such that their respective depletion zones start to overlap, the available volume for the polymer increases. This extra volume in turn causes the total entropy to increase and the free energy to decrease. The colloidal particles experience an effective attraction. In other words, if the depletion layers overlap, the osmotic pressure becomes anisotropic and there is a net osmotic force (see Figure 6.7b).

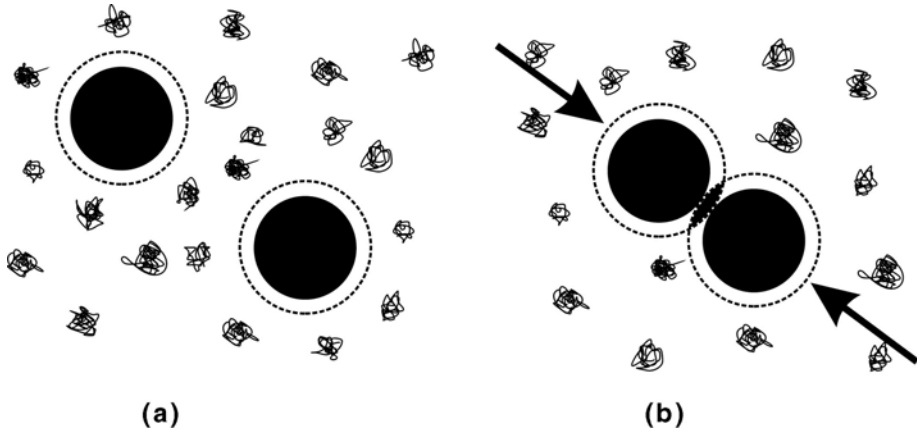

FIGURE 6.7. Schematic representation of two colloidal spheres in a polymer solution with non-adsorbing polymers. The depletion layers are indicated by dashed circles. (a) The osmotic pressure on the spheres due to the polymer solution is isotropic when there is no overlap. (b) The osmotic pressure on the spheres is unbalanced for overlapping depletion layers (the excess pressure is indicated by the arrows).

In the case of binary mixtures of large and small colloidal hard spheres, the depletion potential is in lowest order in the density given by [154,155]

$$\phi(r) = 3k_{\mathrm{B}}T\delta\frac{R}{\sigma}\left(1-\frac{r}{\sigma}\right)^2. \tag{6.10}$$

Here, $k_{\mathrm{B}}T$ is the thermal energy, δ is the volume fraction of the small spheres, R is the radius of the large spheres, σ is the diameter of the small spheres and r is the distance between the surfaces of the two large spheres.

The addition of non-adsorbing polymer to a colloidal suspension induces an interparticle "depletion" attraction whose range and depth can be "tuned" independently by altering the polymer's molecular weight and concentration respectively and could therefore be an extremely helpful tool for the growth of colloidal crystals. The control of attraction due to the density of much smaller particles leads to large crystalline areas in separated phases [156]. In the case of polymer particle several investigations on the phase behaviour were made [157–159] showing useful phase diagrams [159] for crystal growth. A consequence from these phase diagrams is that already at low bead densities the crystallization is initialized when a high concentration of small particles is present in the solvent.

6.3.2. Dynamics in Colloidal Suspensions

6.3.2.1. Gravity and Friction. Optimal fabrication of useful devices often requires an understanding of how to control the crystalline structure by changing the interactions among colloidal spheres, as well as the kinetics of the colloidal spheres. Particles in a suspension are always moving independently due to the Brownian motion. Einstein [156] showed that colloidal particles in a stationary solvent can be regarded as an ideal gas, which results in a diffusion coefficient of a highly diluted system under the assumption that motion through the solvent is connected with the Stokes friction.

However, the suspension additionally experiences gravity. Altogether one has to consider the interaction of gravitational ($F_{\mathrm{g}} = (1/6\pi)\rho_{\mathrm{s}}gd^3$), Archimedes ($F_{\mathrm{A}} = (1/6\pi)\rho_{\mathrm{h}}gd^3$) and frictional forces ($F_{\mathrm{f}} = 3\pi\eta vd$), where ρ_{s} and ρ_{h} are the sphere and solvent mass densities, g is the gravity acceleration, η is the viscosity of the solvent, d is the sphere diameter and $v$is their velocity. When all forces are balanced, the Stokes law is obtained giving directly an expression for the velocity of the silica spheres in the solvent:

$$v = \frac{gd^s}{2\eta}(\rho_{\mathrm{h}} - \rho_{\mathrm{s}}). \tag{6.11}$$

Experimental observations reproduced this expression in an excellent way [160]. Best colloid crystal qualities are obtained for sedimentation speeds between 0.2 and 0.7 mm/h [130]. This can be achieved by appropriate chosen ratio of densities of the silica spheres and the solvent partly compensating the gravitational field. If the suspension is sufficiently diluted the previously discussed attractive and repulsive forces between spheres result in crystallized structures of high order. Especially the formation of the first sedimentation layer was documented in detail by Salvarezza *et al.* [161]. Even at the surface the spheres move by diffusion until they reach their final position. From diffusion theory a distribution probability of spheres can be calculated which then can be used to study

the crystallization of the system. Similar to atomic crystallization the ratio of the total volume and that of all particles in the solvent can be used as a thermodynamic parameter of state in order to describe the phase transition from liquid to solid [162,163]. If this volume ratio exceeds the critical value of 0.49 it will become entropically favourable to establish a long-range order and crystallization starts [164–166]. The crystal structures that have been observed in such systems include bcc, fcc, rhcp and AB_2 [167–177]. When the screening length is shorter than the centre-to-centre distance between two spheres, the colloidal spheres act like "hard spheres" and they will not influence each other until they are in physical contact. In this case, an fcc crystal structure is formed. If the screening length is longer than the centre-to-centre distance, the colloidal spheres behave like "soft" spheres and will only crystallize into a bcc lattice [174–177]. In both crystalline structures, the colloidal spheres are separated by a distance comparable to their size. The disorder-to-order transition can be provoked either by increasing the volume fraction of colloidal spheres or by extending the range of the screening length.

The major disadvantage of the sedimentation method is that it has very little control over the morphology of the top surface and the number of layers of the 3D crystalline arrays [161]. It also takes relatively long periods of time (weeks to months) to completely settle sub-micrometre-sized particles. The 3D arrays produced by the sedimentation method are often polycrystalline. Sedimentation under an oscillatory shear could greatly enhance the crystallinity and ordering in the resulting 3D arrays [178]. In addition to its function as a means for increasing the concentration of colloidal spheres, the gravitational field has a profound effect on the crystalline structure. In a micro-gravity experiment this effect could be eliminated showing that the colloidal spheres were organized into a purely random hexagonal close-packed (rhcp) structure [179].

Figure 6.8 shows a part of a colloidal crystal made from monodisperse silica spheres by sedimentation deposited on a silica glass substrate. The displayed area proves that an

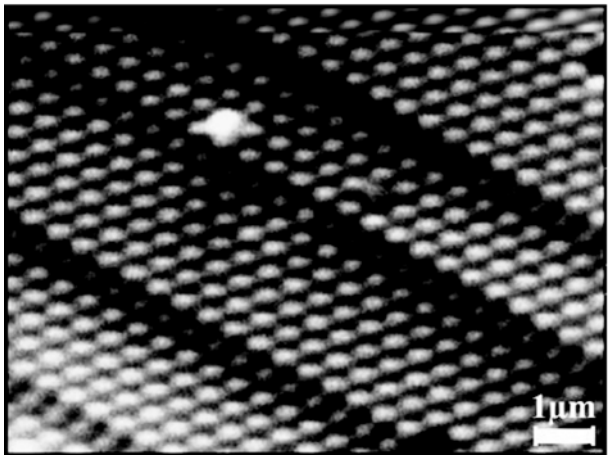

FIGURE 6.8. Electron micrograph of a colloidal crystal made of silica spheres (400 nm diameter) showing an fcc structure. The crystal was grown by sedimentation on a silica glass substrate. The crystalline quality could be improved by applying an external acoustic field [8].

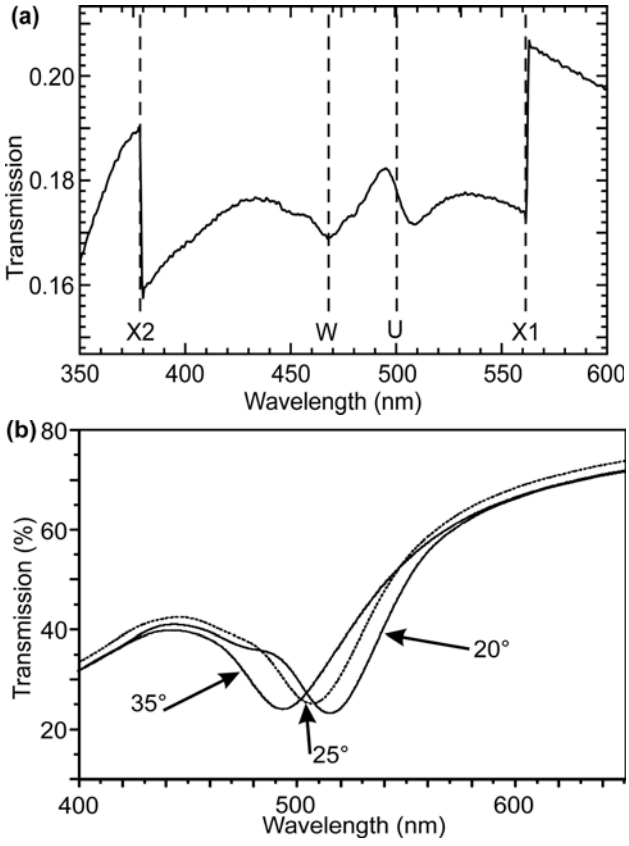

FIGURE 6.9. (a) Transmission spectrum of a polycrystalline colloidal crystal from silica spheres (240 nm diameter) [180]. The sizes of the crystals are at least 20 μm. Since the lattice constants of the colloidal crystals are in the range of the wavelength of the visible light, the transmission spectrum is mainly given by Bragg reflections. Therefore from the transmission spectrum the quality of a colloidal crystal can easily be determined without any damage. The spectrum can be calculated as a superposition of reflections from various differently oriented microcrystals [226]. The notation is given according to directions in k space for an fcc crystal structure. (b) Transmission spectrum of a highly ordered colloidal crystal of silica spheres (230 nm diameter) [8]. The angles are given relative to a ⟨111⟩ direction.

fcc crystal structure is realized. The high crystalline quality was, however, received by applying an external acoustic field [8]. The crystal quality can be controlled with high spatial resolution by electron microscopy as demonstrated in Figure 6.8, which unfortunately is a destructive method. Adapting X-ray diffraction used for the study of crystalline structures of atomic crystals to sub-micrometre lattice elements (silica spheres) visible or ultraviolet light has to be used. One receives similar diffraction images for colloidal crystals as one obtains for atomic crystals, which then allows discriminating amorphous packing, polycrystalline or single crystals. Depending on the light spot used, the desired spatial resolution might be obtained. The spectrum in Figure 6.9a is an example for a low crystalline quality due to numerous differently oriented microcrystals [180]. However, the spectrum of such a polycrystal can be calculated by superposing Bragg reflections

from different orientations of microcrystals with a given crystal structure [89]. In comparison Figure 6.9b shows a spectrum of a colloidal crystal of high crystalline quality [8]. Growing colloidal crystals by sedimentation is a time-consuming procedure, which usually results in a non-adequate crystalline structure as well. As already mentioned above (Figure 6.8) external fields might enhance the crystalline structure, which will be discussed now.

6.3.2.2. External Fields. The precise control of the sedimentation velocity requires additional external fields, which partly compensate gravity and buoyancy. In literature there are numerous examples where electric [111,164,181–183], magnetic [101,103,105,128,182,184–187] or gravity [125,163,164,167,179,188,189] fields were applied.

When an electric field is applied along the gravitation field the velocity of sinking spheres is simply given by Equation (6.11), which is now extended by the electrical mobility μ of the spheres in an electric field E [190]:

$$v = \frac{d^2 g\,(\rho_s - \rho_h)}{2\eta} + \mu E. \tag{6.12}$$

The electrical mobility of the silica spheres can be tuned within certain limit by the pH of the solvent [130]. If the monodisperse SiO_2 nanospheres are of diameters less than 300 nm or more than 550 nm, a controlled crystal growth is usually not successful [130]. If the spheres are too small, the sedimentation rate is very slow or even may not occur. If they are large enough, their sedimentation velocity is such that it is quite hard to achieve an ordered array, and it becomes completely impossible if the diameter is further increased. It is known that when the gravitational energy is much larger than the thermal energy ($k_B T$), the sedimentation occurs far from equilibrium and noncrystalline sediment is obtained. The application of electric fields on charged particles (electrophoresis) [130,164,191], or on uncharged particles (dielectrophoresis) [192–194], allows a precise control of the sedimentation velocity and was investigated in detail by several authors.

Colloidal crystal formation can also be directed by magnetic forces [101,195]. Mainly magnetic fields are used for arraying composite magnetic core-shell particles, where the shell consists of magnetite (Fe_3O_4) nanoparticles with a typical diameter of 10 nm. Because of their single domain nature, these particles bear a permanent magnetic dipole. The energy of one such dipole in the field of a strong permanent magnet is large enough to align these dipoles almost completely with the field. Moreover, the magnetic attraction energy between two magnetic particles is expected to have a noticeable influence on the phase behaviour of a colloidal suspension.

If the silica spheres are too small, resulting in an unacceptable small sedimentation velocity, additional forces are needed in order to reduce the time required for crystal growth. Besides applying an electrical field, moderate acceleration in a centrifugal field is an alternative [118,126,127]. The crystal quality obtained can be optimized by additionally applying ultrasonic. The acoustic field, either phase, frequency or amplitude modulated, acts as a "macroscopic" temperature and supports diffusion during acceleration forced sedimentation. It should be noted that ultrasonic density modulation of the

suspension should act only outside the solid phase; otherwise the solid phase would be "heated" again.

6.3.2.3. Self-Assembly by Capillary Forces. So far the forces and methods described have been mainly used to grow bulk crystals. For the use of photonic applications thin opal layers might be sufficient. Thin opal films can be deposited on a flat substrate by a controlled evaporation of the solvent containing a diluted solution of silica spheres. Experimentally this can be achieved either due to lowering the solvent level by cautiously evaporating the solvent or by slowly lifting the substrate such that at the solvent surface a moving meniscus is induced between the spheres (dip coating). However, the quality of the opaline layers received depends strongly on the relative densities of the solvent and the silica spheres, because when using this method sedimentation should be restricted. One is then left with forces acting between the particles only. At the surface of the colloidal suspension capillary forces, strictly speaking the minimization of the surface energy, result in an attractive force between the spheres [196,197]. The sum of attractive capillary forces acting between the spheres is large compared to the forces between particles described above. Since the surface of the solvent between the spheres is enlarged due to the bend meniscus, the evaporation is enhanced between the spheres, thus a convective flux into the direction of the interacting spheres attracts further particles. This results in self-organized growing clusters of silica spheres at the solvent surface [196,198–203]. By controlling the solvent evaporation rate the flux of the particles moving to the growing colloidal clusters can be controlled. Thus the crystalline quality can be optimized by critically choosing an appropriate balance between particle diffusion and crystallization. As one would expect the particle flux as well as the evaporation of the solvent also depends on the temperature. Additional external fields such as ultrasonic or electrical fields can be used to optimize the crystal structure. Nevertheless, this method is mainly used to grow thin colloidal layers, at least monolayers of silica spheres. Besides the probability of moving the solvent surface by evaporation or moving the substrate, in principle, there are two further choices concerning the orientation of the substrate, namely vertical [190,204] and horizontal orientations. Apart from better crystallinity the vertical alignment allows us to vary the number of monolayers simply by changing the bead concentration in the suspension [204]. Application of alternating external force during the crystallization of the colloid, particularly, shear alignment, has been suggested to enhance the crystallinity and to produce large-area ($\sim$cm^2) defect-free opaline crystals [205]. There are a few experiments to further improve the crystal quality [205] using the vertical deposition method, such as experiments on the effect of the evaporation temperature [206]. The growth of colloidal crystals from aqueous solution can be proceeded at a higher evaporation temperature than that from an ethanolic solution; however, the crystal growth rate is lower. It is found that colloidal crystals grown at a higher evaporation temperature ($\sim>55\,^{\circ}$C) show an increasing tendency towards an equilibrium fcc phase, and also have fewer dislocations and vacancies [206].

Thick layers or bulk colloidal crystals are also obtained with a multiple dip coating. Recently, the capability and feasibility of this method in forming 3D opal lattices with well-controlled numbers of layers along the [111] direction were demonstrated [190].

6.3.3. Alignment Under Physical Confinement

Monodispersed colloidal spheres often organize themselves into a highly ordered 3D structure when they are subjected to a physical confinement [173,207,208]. Recently with such a method 3D opal arrays of colloidal spheres could be produced with domain sizes as large as several square centimetres [209–211]. Colloidal spheres (regardless of the forces between spheres, see above) were assembled by gas pressure into a highly ordered structure in a specially designed packing cell. A continuous sonication was the key to the success of this relatively fast method.

Generally for the fabrication of more controlled crystalline arrays, self-assembly of colloidal spheres on a patterned substrate represents a promising method [212]. A patterned substrate has two kinds of geometrical parameters: the periodicity of the pattern and the surface modulation depth or height of the pattern. Several research groups reported on the effects of the periodicity of the pattern on the crystal array [213,214]. It was demonstrated that colloidal crystallization is greatly affected by the ratio of the surface modulation depth or height to the colloid diameter [188]. Especially there is a large effect of the colloidal array on an imprinted substrate [215].

The physical confinement approach combines templating and attractive inter-sphere forces to self-assemble monodispersed nanospheres into complex aggregates with well-controlled sizes, shapes and internal structures [212,215–217]. For example, the use of patterned arrays of relieves on solid substrates to grow colloidal crystals [188,213,218–220] having unusual crystalline orientations and/or structures [221] was demonstrated. Other examples are patterned monolayers directing the deposition of colloidal particles onto designated regions on a solid substrate [215,222,223].

6.4. THREE-DIMENSIONAL PERIODIC NANOPOROUS MATERIALS

Highly ordered 3D structures of monodisperse colloidal spheres made by techniques described above are themselves particularly suitable candidates as templates for highly ordered porous structures. The colloidal 3D structure as a template simply serves as a scaffold around which other kinds of materials are synthesized. After removal of the template an inverted structure remains. The porous materials obtained are called "inverted opals" (see above).

Such a template-directed synthesis is a convenient and versatile method for generating nanoporous materials. Templating against opal arrays of colloidal spheres offers a generic route to nanoporous materials that exhibit precisely controlled pore sizes and highly ordered 3D nanoporous structures [114–116,118,209,224] and has been successfully applied to their fabrication from a wide variety of materials, including organic polymers, ceramic materials, inorganic semiconductors and metals [27,114–116,118–124,225,209,226–230]. The fidelity of this procedure is mainly determined by the quality of the colloidal sphere template, kinetic factors such as the filling void spaces in the template and the volume shrinkage of precursors during solidification (usually by drying or heating).

For the realization of such structures several procedures have been developed. After drying the opal array of colloidal spheres, the void spaces among the colloidal spheres

are infiltrated with a liquid precursor such as a dispersion of nanoparticles [228], a solution containing an inorganic salt [119], an ultraviolet or thermally curable organic prepolymer [116,117,209], an ordinary organic monomer [27] or a sol–gel precursor to a ceramic material [27,114–116,118,209,224–227]. Subsequent solidification of the precursor and removal of the colloidal spheres results in a 3D nanoporous structure with a highly ordered architecture of uniform air spheres, interconnected to each other by small circular windows. The void spaces among colloidal spheres have also been filled with a variety of materials through electrochemical deposition [121,123] or by chemical vapour deposition (CVD), with which the degree of filling can be accurately controlled. Thus, CVD was used to fill silica crystals with graphite and diamond [224], silicon [231] and germanium [232]. However, a difficulty is the obstruction with material of the outermost channels which provide access to the innermost channels. By low-pressure CVD, which prevented channel obstruction, and highly ordered silica crystals, inverted crystals of silicon were fabricated [233]. Similarly, a liquid phase deposition process can be used if the deposition occurs under mild conditions and results in conformal hydrous films growing the inverted structure [29].

In the next step the colloidal template is removed from its solidified environment by dissolution, evaporation or firing at temperatures of up to 400 °C. This final step often also involves calcination of the material at elevated temperatures in order for the resulting porous framework to densify and crystallize.

Figure 6.10 shows an inverted opal made from a highly ordered silica nanosphere template which was infiltrated with TiO_2 nanocrystals [226]. The TiO_2 nanocrystals were

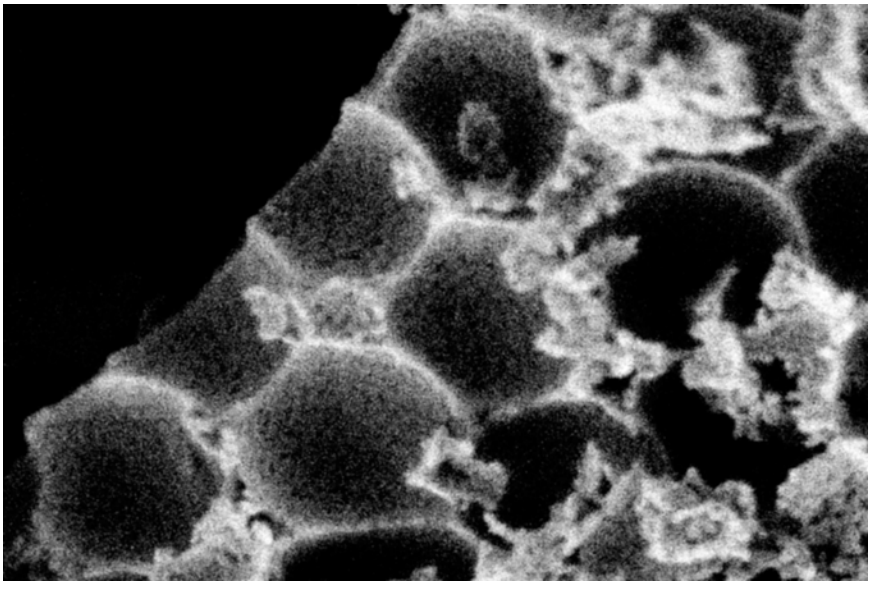

FIGURE 6.10. The inverted opal structure was made from a highly ordered silica nanosphere template infiltrated with TiO_2 nanocrystals, which were grown by a sol–gel process. After infiltration, heating for solidification and removal of the template the inverted structure remains. The size of the TiO_2 nanocrystals is typically up to 10 nm [226].

grown by a sol–gel process [4]. After infiltration, heating for solidification and removal of the template the inverted structure remains, showing the polycrystalline structure of TiO_2 nanocrystals with sizes up to 10 nm (see Figure 6.10).

The fabrication of nanoporous materials based on this approach is not only remarkable for its simplicity, and for its degree of accuracy in transferring 3D nanostructures from the template to the replica, but also a cost-effective and high-throughput procedure. The size of the pores and the periodicity of the porous structures can be precisely controlled and easily tuned by changing the size of the colloidal template spheres. A similar approach is extensible to a large variety of materials. The only requirement seems to be the availability of a precursor that can infiltrate into the void spaces among colloidal spheres without significantly swelling or dissolving the template.

6.5. APPLICATIONS

Colloidal particles have been extensively studied in the context of materials science, condensed matter physics, chemistry, biology, medicine and applied optics [169,234,235]. They have long been used as major components of numerous industrial products such as inks, paints, toners, coatings, foods, drinks, cosmetics or photographic films [149,236,237]. Spherical colloids have been the dominant subject of research for many decades due to their ease of production as monodispersed spheres [238–240] and the wide variety of chemical methods developed to generate them from a range of different materials [6,36,241–243]. Spherical colloids can be readily self-assembled into three-dimensionally ordered lattices such as colloidal crystals or synthetic opals [167,168,244]. The ability to crystallize spherical colloids into spatially periodic structures has allowed us to obtain interesting and often useful functionality not only from the colloidal materials but also from the long-range order exhibited by these crystalline lattices [76,176,177,245]. Until now numerous applications for colloidal particles are known; however, so far only a few applications have been established for colloidal crystals. Materials with spatially ordered features on the nanometre scale have, however, current and future potential applications in optical or magnetical information processing and storage, advanced coatings, catalysis and other emerging nanotechnologies. The long-range ordering of the colloidal particles results in a number of distinctive and potentially useful characteristics such as optical diffraction and photonic bandgaps. Studies on the optical properties of these materials have now evolved into a new and active field of research that is often referred to as photonic crystals or photonic bandgap structures [27,114,116,118,121–124,127,228–231,246,247]. The reader who is interested in the background on the physics of photonic crystals is referred to textbooks and monographs [248–252].

There are also biological applications of colloidal nanocrystals reported [253], for example, the use of nanostructured materials as artificial bones [254], as fluorescent probes to label cells [25,255–263] and chemical libraries [264–266].

Monolayers of magnetic monodisperse core-shell colloids are currently under investigation for their application to ultra-high-density magnetic storage devices [267–270]. Chemical techniques have been used to form silica coatings on nanoparticles of various

materials including nickel [271], iron [272–274], iron oxide [275–277] and a nickel/iron composite [274]. Because of the large surface area to volume ratio of nanospheres, coating by magnetic materials is less favourable because metallic nanoparticles are hampered by issues of chemical stability, dispersion and surface functionalization. They are susceptible to attack by oxidative or corrosive environments that may alter their chemistry and diminish their properties, thus they have to be protected by additional coating.

In nanosphere lithography technique the self-assembly of single layer and double layer of nanospheres is used forming a hexagonally close-packed crystal for the deposition of material through this colloidal crystal mask, with subsequent removal of the nanospheres, resulting in an array of evenly spaced, homogeneous nanoparticles [278–281]. The dimension of these truncated periodic nanoparticle arrays can be easily tuned by choice of nanosphere diameter. Nanosphere lithography can be envisioned for applications such as fundamental studies of material properties as a function of particle size, quantum dot arrays [282–284], single-electron transistors and the electrochemistry of nanometre-sized structures (e.g., high-T_c Josephson effect devices [285]).

Dried colloidal crystals are very brittle and may disperse in water. Any practical device thus requires that the crystal either be fixed in place or replicated by another more robust material. Indeed, nature's opals are an example of fixing. A colloidal crystal of silica spheres is made into a solid material after infiltrating the voids between the particles by hydrated silica. Within a few years the fabrication of porous materials using colloidal crystal templates has become a rapidly growing field. Nearly all classes of inorganic and organic materials and metals have been templated into porous ordered structures. The creation of these structures is a fascinating and intellectually challenging problem, but interest in these materials also arises from their wide array of potentially usable applications. One of the most "visible" applications is photonic crystals. Such crystals could increase the efficiency of light emitting diodes and be used in optical processing devices as integrated optical miniature waveguides [286,287], filters and resonators, microcavity lasers [288], mirrors or optical chips [220], thereby acting as analogs to semiconductors in electric circuits [248].

Structured porous materials (inverted opals) can possess desired full photonic bandgaps when created out of a matrix with high refractive index [121,127,228,229, 248,289]. However, such materials have not yet been synthesized, even though recent advances in creating structures via electrochemical growth of semiconductors appear very promising [248].

Apart from photonic crystals and optical applications, the three-dimensional porous materials have potential applications in advanced catalysis, where the hierarchical porosity combines efficient transport and high surface area. Both the bulk and surface chemistry of the materials can be modified to the desired composition [29,118,119]. Interesting catalytic and other applications could be based on the ability of the method to form membranes or composite metallic/dielectric structures. This new field is clearly far from exhausting its store of novel ideas and possibilities [28]. An interesting application could also be photocatalysis (see, e.g., [290]) either when using inverted opals for collecting light or by using directly inverted opals made from semiconductors.

6.6. CONCLUDING REMARKS

Although a variety of preparation methods have been developed, the creation of high quality periodic 3D porous structures, preferably over large areas, uniformly and at low cost, is still a challenging problem. Problems associated with template assisted fabrication of porous structures include preparation of a high quality template, complete filling of the voids in the template and the minimization of shrinkage upon template removal by heating or etching. Since any of these factors can influence the final quality of the porous structure, all these requirements must be fulfilled at the same time.

Devices based on porous titania such as photo-voltaic cells, gas sensors or electrochromic displays have attracted considerable attention in recent years. The efficiency of such devices is enhanced by a precise control of pore size and distribution. Sol–gel fabrication routes offer both low cost and great flexibility in the fabrication of periodic porous 3D structures.

REFERENCES

[1] E. Matijevic, Monodispersed metal (hydrous) oxides—a fascinating field of colloid sciences, Acc. Chem. Res. **14**, 22–29 (1981).
[2] E. Matijevic, Monodispersed colloids: art and science, Langmuir **2**, 12–20 (1986).
[3] C. Feldmann, Preparation of nanoscale pigment particles, Adv. Mater. **13**, 1301–1303 (2001).
[4] C.J. Brinker, *Sol-Gel-Science*, Academic Press, New York, 1990.
[5] H.E. Bergna (Ed.), *Adv. Chem. Series: The Colloid Chemistry of Silica*, Vol. 234, American Chemical Society, Washington, DC, 1994.
[6] W. Stoeber, A. Fink and E. Bohn, Controlled growth of monodisperse silica spheres in the micron size range, J. Colloid Interface Sci. **26**, 62 (1968).
[7] G. De, B. Karmakar and D. Ganguli, Controlled growth of monodisperse silica spheres in the micron size range, J. Mater. Chem. **10**, 2289–2293 (2000).
[8] H. Winkler, Synthese und charakterisierung photonischer bandlückenmaterialien, Diploma thesis, Paderborn, Germany, 2001.
[9] M. Dresselhaus, G. Dresselhaus and P. Avouris, *Carbon Nanotubes*, Springer, Berlin, 2000.
[10] K. Shelimov and M. Moskovits, Composite nanostructures based on template-grown boron nitride nanotubules, Chem. Mater. **12**, 250 (2000).
[11] O. Lourie, C. Jones, B. Bartlett, P. Gibbons, R. Ruoff and W. Buhro, CVD growth of boron nitride nanotubes, Chem. Mater. **12**, 1808 (2000).
[12] R. Ma, Y. Bando, T. Sato and K. Kurashima, Growth, morphology, and structure of boron nitride nanotubes, Chem Mater. **13**, 2965 (2001).
[13] Z. Zhang, B. Wei, J. Ward, R. Vajtai, G. Ramanath and P. Ajayan, Select pathways to carbon nanotube film growth, Adv. Mater. **13**, 1767 (2001).
[14] Y. Sui, D. Acosta, J. Gonzalez-Leon, A. Bermudez, J. Feuchtwanger, B. Cui, J. Flores and M. Saniger, Structure, thermal stability and deformation of multibranched carbon nanotubes synthesized by CVD in the AAO template, J. Phys. Chem. B **105**, 1523 (2001).
[15] A. Peigney, P. Coquay, E. Flahaut, R. Vandenberghe, E. De Grave and C. Laurent, A study of the formation of single- and double-walled carbon nanotubes by a CVD method, J. Phys. Chem. B **105**, 9699 (2001).
[16] A. Morales and C. Lieber, A laser ablation method for the synthesis of crystalline semiconductor nanowires, Science **279**, 208 (1998).
[17] J. Holmes, K. Johnston, R. Doty and B. Korgel, Control of the thickness and orientation of solution-grown silicon nanowires, Science **287**, 1471 (2000).
[18] D. Al-Mawlawi, C.Z. Liu and M. Moskovits, Nanowires formed in anodic oxide nanotemplates, J. Mater. Res. **9**, 1014 (1994).

[19] J.C. Hulteen and C.R. Martin, A general template-based method for the preparation of nanomaterials, J. Mater. Chem. **7**, 1075–1087 (1997).
[20] G. Che, B. Lakshmi, C. Martin, E. Fisher and R. Ruoff, Chemical vapor deposition (CVD)-based synthesis of carbon nanotubes and nanofibers using a template method, Chem. Mater. **10**, 260 (1998).
[21] H. Masuda, T. Yanagishita, K. Yasui, K. Nishio, I. Yagi and A. Fujishima, Synthesis of well-aligned diamond nanocylinders, Adv. Mater. **13**, 247 (2001).
[22] L. Cao, Z. Zhang, L. Sun, C. Gao, M. He, Y. Wang, Y. Li, X. Zhang, G. Li, J. Zhang and W. Wang, Well-aligned boron nanowire arrays, Adv. Mater. **13**, 1701–1704 (2001).
[23] A.P. Alivisatos, Perspectives on the physical chemistry of semiconductor nanocrystals, J. Phys. Chem. **100**, 13226–13239 (1996).
[24] C. Wang, M. Shim and P. Guyot-Sionnest, Electrochromic nanocrystal quantum dots, Science **291**, 2390 (2001).
[25] M.J. Bruchez, M. Moronne, P. Gin, S. Weiss and A.P. Alivisatos, Semiconductor nanocrystals as fluorescent biological labels, Science **281**, 2013–2016 (1998).
[26] Y. Vlasov, X. Bo, J. Sturm and D. Norris, On-chip natural assembly of silicon photonic bandgap crystals, Nature **414**, 2425 (2001).
[27] S.A. Johnson, P.J. Ollivier and T.E. Mallouk, Ordered mesoporous polymers of tunable pore size from colloidal silica templates, Science **283**(12), 963–965 (1999).
[28] O.D. Velev and E.W. Kaler, Structured porous materials via colloidal crystal templating: from inorganic oxides to metals, Adv. Mater. **12**(7), 531–534 (2000).
[29] S. Nishimura, A. Shishido, N. Abrams and T.E. Mallouka, Fabrication technique for filling-factor tunable titanium dioxide colloidal crystal replicas, Appl. Phys. Lett. **81**(24), 4532–4534 (2002).
[30] O.D. Velev and A.M. Lenhoff, Colloidal crystals as templates for porous materials, Curr. Opin. Colloid Interface Sci. **5**, 56–63 (2000).
[31] S. Polarza and B. Smarslya, Nanoporous materials, J. Nanosci. Nanotechnol. **2**, 581–612 (2002).
[32] G.H. Bogush, M.A. Tracy and C.F. Zukoski, Preparation of monodisperse silica particles: control of size and mass fraction, J. Non-Cryst. Solids **104**, 95 (1988).
[33] A. Burneau and B. Humbert, Aggregative growth of silica from an alkoxysilane in a concentrated solution of ammonia, Colloids Surf. A **75**, 111 (1993).
[34] H. Giesche, Synthesis of monodispersed silica powders: I. Particle properties and reaction kinetics, J. Eur. Ceram. Soc. **14**, 189 (1994).
[35] H. Giesche, Synthesis of monodispersed silica powders: II. Controlled growth reaction and continuous production process, J. Eur. Ceram.Soc. **14**, 205 (1994).
[36] F. Candau and R.H. Ottewill, *An Introduction to Polymer Colloids*, Kluwer, Dordrecht, the Netherlands, 1990.
[37] J. Ugelstad, M.S. Elaasser and J. Vanderhoff, The acid decomposition of methylol melamines and methoxymethyl melamines, J. Polym. Sci. Part C: Polym. Lett. **11**, 503–513 (1973).
[38] J.W. Goodwin, J. Hearn, C.C. Ho and R.H. Ottewill, Preparation and characterization of monodisperse polystyrene latexes: III. Preparation without added surface active agents, Colloid Polym. Sci. **252**, 464 (1974).
[39] L. Antl, J.W. Goodwin, R.D. Hill, R.H. Ottewill, S.M. Owens, S. Papworth and J.A. Waters, The preparation of poly(methyl methacrylate) lattices in non-aqueous media, Colloids Surf. **17**, 67 (1986).
[40] C.M. Tseng, Y.Y. Lu, M.S. El Aasser and J.W. Vanderhoff, Uniform polymer particles by dispersion polymerization in alcohol, J. Polym. Sci., Polym. Chem. **24**, 2995 (1986).
[41] G.T.D. Shouldice, G.A. Vandezande and A. Rudin, Practical aspects of the emulsifier-free emulsion polymerization of styrene, Eur. Polym. J. **30**, 179 (1994).
[42] C.E. Reese, C.D. Guerrero, J.M. Weissman, K. Lee and S.A. Asher, Synthesis of highly charged, monodisperse polystyrene colloidal particles for the fabrication of photonic crystals, J. Colloid Interface Sci. **232**, 76 (2000).
[43] C. Feldmann and H.-O. Jungk, Polyol-vermittelte Präparation nanoskaliger Oxidpartikel, Angew. Chemie **113**, 372–374 (2001).
[44] C.R. Silva and C. Airoldi, Acid and base catalysts in the hybrid silica sol-gel process, J. Coll. Interf. Sci. **195**, 381–387 (1997).
[45] A. van Blaaderen and A. Vrij, Synthesis and characterization of monodisperse colloidal organo-silica spheres, J. Colloid Interface Sci. **156**, 1–18 (1993).

[46] A. van Blaaderen and A.P.M. Kentgens, Particle morphology and chemical microstructure of colloidal silica spheres made from alkoxisilanes, J. Non-Cryst. Solids **149**, 161–178 (1992).
[47] T. Matsoukas and E. Gulari, Monomer-addition growth with a slow initiation step: a growth model for silica particles from alkoxides, J. Colloid Interface Sci. **132**, 13–21 (1989).
[48] T. Matsoukas and E. Gulari, Dynamics of growth of silica particles from ammonia-catalyzed hydrolysis of TEOS, J. Colloid Interface Sci. **124**, 252–261 (1988).
[49] G.H. Bogush and C.F. Zukoski, Studies of the kinetics of the precipitation of uniform silica particles through the hydrolysis and condensation of silicon alkoxides, IV, J. Colloid Interface Sci. **142**, 1–18 (1991).
[50] T. Okubo, K. Kobayashi, A. Kuno and A. Tsuchida, Kinetic study of the formation reaction of colloidal silica spheres in microgravity using aircraft, Colloid Polym. Sci. **277**, 483–487 (1999).
[51] J.K. Bailey and M.L. Mecartney, Formation of colloidal silica particles from alkoxides, Colloids Surf. **63**, 131–138 (1992).
[52] S.L. Chen, P. Dong and G.-H. Yang, The size dependence of growth rate of monodisperse silica particles from tetraalkoxysilane, J. Colloid Interface Sci. **189**, 268–272 (1997).
[53] C.J.J. den Ouden and R.W. Thompson, The size dependence of growth rate of monodisperse silica particles from tetraalkoxysilane, J. Colloid Interface Sci. **143**, 77–84 (1991).
[54] K.P. Velikov and A. van Blaaderen, Synthesis and characterization of monodisperse core-shell colloidal spheres of zinc sulfide and silica, Langmuir **17**, 4779–4786 (2001).
[55] C. Blum, Ph.D. thesis, Paderborn, Germany, 2004.
[56] F. Baumann, M. Schmidt, B. Deubzer, M. Geek and J. Dauth, On the preparation of organosilicon m-spheres: a polycondensation in m-emulsion, Macromolecules **27**, 6102–6105 (1994).
[57] D.B. Zhang, H.M. Cheng, J.M. Ma, Y.P. Wang and X.Z. Gai Synthesis of silver-coated silica nanoparticles in nonionic reverse micelles, J. Mater. Sci. Lett. **20**, 439–440 (2001).
[58] J. Esquena, Th. F. Tadros, K. Kostarelos and C. Solans, Preparation of narrow size distribution silica particles using microemulsions, Langmuir **13**, 6400–6406 (1997).
[59] R.I. Nooney, D. Thirunavukkarasu, Y. Chen, R. Josephs and A.E. Ostafin, Synthesis and nanoscale mesoporous silica spheres with controlled particle size, Chem. Mater. **14**(11), 4721–4728 (2002).
[60] Q. Cai, F.Z. Cui, X.H. Chen, Y. Zhang and Z.S. Luo, Nanosphere of ordered silica MCM-41 hydrothermally synthesized with low surfactant concentration, Chem. Lett. **2000**, 1044–1045 (2000).
[61] L. Wang, S. Velu, S. Tomura, F. Ohashi and K. Suzuki, Synthesis and characterization of CuO containing mesoporous silica spheres, J. Mater. Sci. **37**, 801–806 (2002).
[62] A.K. van Helden and A. Vrij, Contrast variation in light scattering: silica spheres dispersed in apolar solvent mixtures, J. Colloid Interface Sci. **76**, 418–433 (1980).
[63] A.K. van Helden, J.W. Jansen and A. Vrij, Preparation and characterization of spherical monodisperse silica dispersions in nonaqueous solvents, J. Colloid Interface Sci. **81**, 354–368 (1981).
[64] K. Bridger, D. Falkenhurst and B. Vincent, Nonaqueous silica dispersions stabilized by terminally-grafted polystyrene chains, J. Colloid Interface Sci. **68**, 190–195 (1979).
[65] H. de Hek and A. Vrij, Preparation of sterically stabilized silica dispersions in nonaqueous media, J. Colloid Interface Sci. **79**, 289–294 (1981).
[66] A. Imhof, M. Megens, J.J. Engelberts, D.T.N. de Lang, R. Sprick and W.L Vos, Spectroscopy of fluorescein (FITC) dyed colloidal silica spheres, J. Phys. Chem. B **103**, 1408–1415 (1999).
[67] A. van Blaaderen and A. Vrij, Synthesis and characterization of colloidal dispersions of fluorescent, monodisperse silica spheres, Langmuir **8**, 2921–2931 (1992).
[68] S. Kang, S. Il Hong, C.R. Choe, M. Park, S. Rim and J. Kim, Preparation and characterization of epoxy composites filled with functionalized nanosilica particles obtained via sol-gel process, Polymer **42**, 879–887 (2001).
[69] O.C. Monteiro, A.C.C. Esteves and T. Trindade, The synthesis of SiO_2@CdS nanocomposites using single-molecule precursors, Chem. Mater. **14**, 2900–2909 (2002).
[70] C.E. Moran, G.D. Hale and N.J. Halas, Synthesis and characterization of lanthanide-doped silica microspheres, Langmuir **17**, 8376–8379 (2001).
[71] M.J.A. de Dood, B. Berhout, C.M. van Kats, A. Polman and A. van Blaaderen, Acid-based synthesis of monodisperse rare-earth-doped colloidal SiO_2 spheres, Chem. Mater. **14**, 2849–2853 (2002).
[72] W. Wang and S.A. Asher, Photochemical incorporation of silver quantum dots in monodisperse silica colloids for photonic crystal applications, J. Am. Chem. Soc. **123**, 12528–12535 (2001).

[73] L.M. Liz-Marzán, M.A. Correa-Duarte, I. Pastoriza-Santos, P. Mulvaney, T. Ung, M. Giersig and N.A. Kotov, Core shell nanoparticles and assemlies thereof, in *Handbook of Surfaces and Interfaces of Materials*, Ed. H.S. Nalwa, Academic Press, San Diego, USA, 2001, Chapter 5.
[74] F. Caruso, Nanoengineering of particle surfaces, Adv. Mater. **13**(1), 11–22 (2001).
[75] N.A.M. Verhaegh and A. van Blaaderen, Dispersions of rhodamine labeled silica spheres: synthesis, characterization, and fluorescence confocal scanning laser microscopy, Langmuir **10**, 1427–1438 (1994).
[76] S.Y. Chang, L. Liu and S.A. Asher, Creation of templated complex topological morphologies in colloidal silica, J. Am. Chem. Soc. **116**, 6745–6747 (1994).
[77] L.M. Liz-Marzan, M. Giersig and P. Mulvaney, Synthesis of nanosized gold-silica core-shell particles, Langmuir **12**, 4329 (1996).
[78] C. Graf, W. Schärtl, K. Fischer, N. Hugenberg and M. Schmidt, Dye-labeled poly(organosiloxane) microgels with core-shell architecture, Langmuir **15**, 6170–6180 (1999).
[79] K.P. Velikov, A. Moroz and A. van Blaaderen, Photonic crystals of core-shell colloidal particles, Appl. Phys. Lett. **80**, 49–51 (2002).
[80] W. Strek, P.J. Deren, E. Lukowiak, J. Hanuza, H. Drulis, A. Bednarkiewicz and V. Gaishun, Spectroscopic studies of chromium-doped silica sol-gel glasses, J. Non-cryst. Solids **288**, 56–65 (2001).
[81] S. Ramesh, Y. Cohen, D. Aurbach and A. Gedanken, AFM investigation of the surface topography and adhesion of nickel nanoparticles to submicrospherical silica, Chem. Phys. Lett. **287**, 461–467 (1998).
[82] V.B. Prokopenko, V.S. Gurin, A.A. Alexeenko, V.S. Kulikauskas and D.L. Kovalenko, Surface segregation of transition metals in sol-gel silica films, J. Phys. D: Appl. Phys. **33**, 3152–3155 (2000).
[83] C.F. Song, M.K. Lü, P. Yang, D. Xu and D.R. Yuan, Study on the photoluminescence properties of sol-gel Ti^{3+} doped silica glasses, J. Sol-Gel Sci. Technol. **25**, 113–119 (2002).
[84] S.M. Jones and S.E. Friberg, Charge transfer transitions of copper (II) in drying silicate xerogels, Phys. Chem. Glasses **37**(3), 111–115 (1996).
[85] M. Nofz, R. Stösser, B. Unger and W. Herrmann, The function of paramagnetic iron species in amorphous materials formed by sol-gel method and conventional melting techniques, J. Non-Cryst. Solids **149**, 62–76 (1992).
[86] M.A. Villegas, M.A. Garcia, J. Llopis and J.M. Fernandez Navarro, Optical spectroscopy of hybrid sol-gel coatings doped with noble metals, J. Sol-Gel Sci. Technol. **11**, 251–265 (1998).
[87] B. Friedel, Dotierung von Siliziumdioxid-Kugeln für photonische Anwendungen, Diploma thesis, Paderborn, Germany, 2003.
[88] Y. Sun and Y. Xia, Alloying and dealloying processes involved in the preparation of metal nanoshells through a galvanic replacement reaction, Nano Lett. **3**, 1569–1572 (2003).
[89] S. Greulich-Weber and E. Waldmüller, unpublished results.
[90] L.H. Slooff, M.J.A. de Dood, A. van Blaaderen and A. Polman, Erbium-implanted silica colloids with 80% luminescence quantum efficiency, Appl. Phys. Lett. **76**(25), 3682–3684 (2000).
[91] L.H. Slooff, A. van Blaaderen, A. Polman, G.A. Hebbink, S.I. Klink, F.C.J.M. van Veggel, D.N. Reinhoudt and J.W. Hofstraat, Rare-earth doped polymers for planar optical amplifiers, J. Appl. Phys. **91**(7), 3955–3980 (2002).
[92] C. De Julian Fernandez, C. Sangregorio, G. Mattei, G. De, A. Saber, S. Lo Russo, G. Battaglin, M. Catalano, E. Cattaruzza, F. Gonella, D. Gatteschi and P. Mazzoldi, Structure and magnetic properties of alloy-based nanoparticles silica composites prepared by ion-implantation and sol-gel techniques, Mater. Sci. Eng. C **15**, 59–61 (2001).
[93] Y. Takeda, C.G. Lee and N. Kishimoto, Optical properties of nanoparticle composites in insulators by high-flux 60 keV Cu^- implantation, Nucl. Instrum. Methods Phys. Res. B **190**, 797–801 (2002).
[94] D.L. Griscom, E' center in glassy SiO_2: microwave saturation properties and confirmation of the primary ^{29}Si hyperfine structure, Phys. Rev. B **20**, 1823 (1979).
[95] M. Donbrow (Ed.), *Microcapsules and Nanoparticles in Medicine and Pharmacy*, CRC Press, Boca Raton, FL, 1992, Chapters 6 and 16.
[96] R. Langner, New methods of drug delivery, Science **249**, 1527–1533 (1990).
[97] F. Caruso, R.A. Caruso and H. Mohwald, Nanoengineering of inorganic and hybrid hollow spheres by colloidal templating, Science **282**, 1111–1114 (1998).
[98] E.M.B. de Sousa, A.P.G. de Sousa, N.D.S. Mohallem and R.M. Lago, Copper-silica sol-gel catalysts: structural changes of Cu species upon thermal treatment, J. Sol-Gel Sci. Technol. **26**, 873–877 (2003).

[99] I.L. Lyubchanskii, N.N. Dadoenkova, M.I. Lyubchanskii, E.A. Shapovalov and Th. Rasing, Magnetic photonic crystals, J. Phys. D: Appl. Phys. **36**, R277–R287 (2003).
[100] C. Koerdt, G.L.J.A. Rikken and E.P. Petrov, Faraday effect of photonic crystals, Appl. Phys. Lett. **82**(10), 1538–1541 (2003).
[101] E.L. Bizdoacaa, M. Spasovaa, M. Farlea, M. Hilgendorffb and F. Carusoc, Magnetically directed self-assembly of submicron spheres with a Fe_3O_4 nanoparticle shell, J. Magn. Magn. Mater. **240**, 44–46 (2002).
[102] C.B. Murray, Shouheng Sun, W. Gaschler, H. Doyle, T.A. Betley and C.R. Kagan, Colloidal synthesis of nanocrystals and nanocrystal superlattices, IBM J. Res. Dev. **45**(1), 47–56 (2001).
[103] R. Wiesendanger, M. Bode, M. Kleiber, M. Lohndorf, R. Pascal, A. Wadas and D. Weiss, Magnetic nanostructures studied by scanning probe microscopy and spectroscopy, J. Vac. Sci. Technol. B **15**, 1330 (1997).
[104] S. O'Brien and J.B. Pendry, Magnetic activity at infrared frequencies in structured metallic photonic crystals, J. Phys.: Condens. Matter **14**, 6383–6394 (2002).
[105] A.J. Haes, C.L. Haynes and R.P. Van Duyne, Nanosphere lithography: self-assembled photonic and magnetic materials, Mater. Res. Soc. Symp. **636**, D4.8/1–D4.8/6 (2001).
[106] A. Moroz, Photonic crystals of coated metallic spheres, Europhys. Lett. **50**(4), 466–472 (2000).
[107] Y. Jiang, C. Whitehouse, Jensen Li, Wing Yim Tam, C.T. Chan and Ping Sheng, Optical properties of metallo-dielectric microspheres in opal structures, J. Phys.: Condens. Matter **15**, 5871–5879 (2003).
[108] N. Eradata, J.D. Huanga, Z.V. Vardenya, A.A. Zakhidovb, I. Khayrullinb, I. Udodb and R.H. Baughmanb, Optical studies of metal-infiltrated opal photonic crystals, Synth. Met. **116**, 501–504 (2001).
[109] A.P. Philipse, Solid opaline packings of colloidal silica spheres, J. Mater. Sci. Lett. **8**(12), 1371–1373 (1989).
[110] J.V. Sanders, Colour of precious opal, Nature **204**, 1151–1153 (1964).
[111] J. Aizenberg, P.V. Braun and P. Wiltzius, Patterned colloidal deposition controlled by electrostatic and capillary forces, Phys. Rev. Lett. **84**, 2997 (2000).
[112] T.C. Simonton, R. Roy, S. Komarneni and E. Breval, Microstructure and mechanical properties of synthetic opal: a chemically bonded ceramic, J. Mater. Res.**1**, 667 (1986).
[113] V.N. Bogomolov, S.V. Gaponenko, I.N. Germanenko, A.M. Kapitonov, E.P. Petrov, N.V. Gaponenko, A.V. Prokofiev, A.N. Ponyavina, N.I. Silvanovich and S.M. Samoilovich, Photonic band gap phenomenon and optical properties of artificial opals, Phys. Rev. E **55**, 7619–7625 (1997).
[114] O.D. Velev, T.A. Jede, R.F. Lobo and A.M. Lenhoff, Porous silica via colloidal crystallization, Nature **389**, 447 (1997).
[115] O.D. Velev, T.A. Jede, R.F. Lobo and A.M. Lenhoff, Microstructured porous silica obtained via colloidal crystal templates, Chem. Mater. **10**, 3597 (1998).
[116] S.H. Park and Y. Xia, Dimensionally interconnected spherical pores, Adv. Mater. **10**, 1045–1046 (1998).
[117] B. Gates, Y. Yin and Y. Xia, Fabrication and characterization of porous membranes with highly ordered three-dimensional periodic structures, Chem. Mater. **11**, 2827–2836 (1999).
[118] B.T. Holland, C.F. Blanford and A. Stein, Synthesis of highly ordered three-dimensional mineral honeycombs with macropores, Science **281**, 538–540 (1998).
[119] H. Yan, C.F. Blanford, B.T. Holland, M. Parent, W.H. Smyrl and A. Stein, A general chemical synthesis of periodic macroporous metals, Adv. Mater. **11**, 1003–1006 (1999).
[120] O.D. Velev, P.M. Tessier, A.M. Lenhoff and E.W. Kaler, A class of porous metallic nanostructures, Nature **401**, 548 (1999).
[121] P.V. Braun and P. Wiltzius, Electrochemically grown photonic crystals, Nature **402**, 603–604 (1999).
[122] P.N. Bartlett, T. Dunford and M.A. Ghanem, Templated electrochemical deposition of nanostructured macroporous PbO_2, J. Mater. Chem., **12**, 3130–3135 (2002).
[123] P. Jiang, J. Cizeron, J.F. Bertone and V.L. Colvin, Preparation of macroporous metal films from colloidal crystal, J. Am. Chem. Soc. **121**, 7957–7958 (1999).
[124] P. Yang, T. Deng, D. Zhao, P. Feng, D. Pine, B.F. Chmelka, G.M. Whitesides and G.D. Stucky, Hierarchically ordered oxides, Science **282**, 2244–2246 (1998).
[125] H. Miguez, F. Meseguer, C. Lopez, A. Blanco, J. Moya, J. Requena, A. Mifsud and V. Fornes, Control of the photonic crystal properties of fcc-packed submicrometer SiO_2 spheres by sintering, Adv. Mater. **10**, 480–483 (1998).

[126] S. Tsunekawa, Y.A. Barnakov, V.V. Poborchii, S.M. Samoilovich, A. Kasuya and Y. Nishina, Characterization of precious opals: AFM and SEM observations, photonic band gap, and incorporation of CdS nano-particles, Microporous Mater. **8**, 275 (1997).
[127] J. Wijnhoven and W.L. Vos, Preparation of photonic crystals made of air spheres in titania, Science **281**, 802–804 (1998).
[128] M. Trau, D.A. Saville and I.A. Aksay, Field-induced layering of colloidal crystals, Science **272**, 706 (1996).
[129] M. Trau, D.A. Saville and I.A. Aksay, Assembly of colloidal crystals at electrode interfaces, Langmuir **13**, 6375–6381 (1997).
[130] M. Holgado, F. Garcia-Santamaria, A. Blanco, M. Ibisate, A. Cintas, H. Miguez, C.J. Serna, C. Molpeceres, J. Requena, A. Mifsud, F. Meseguer and C. Lopez, Electrophoretic deposition to control artificial opal growth, Langmuir **15**, 4701–4704 (1999).
[131] O. Stern, Zur Theore der elektrischen Doppelschicht, Z. Elektrochem. **30**, 508 (1924).
[132] J.N. Israelachvili, *Intermolecular and Surface Forces*, Academic Press, London and New York, 1992.
[133] M. Elimelech, J. Gregory, X. Jia and R.A. Williams, *Particle Deposition and Aggregation: Measurement, Modeling, and Simulation*, Butterworth, Oxford, 1995.
[134] J. Gregory, Interaction of unequal double layers at constant charge, J. Colloid Interface Sci. **51**, 44–51 (1975).
[135] G.M. Bell, S. Levine and L.N. McCartney, Approximate methods of determining the double-layer free energy of interaction between two charged colloid spheres, J. Colloid Int. Sci.**33**, 335 (1970).
[136] A.K. Arora and B.V.R. Tata (Eds.), *Ordering and Phase Transitions in Charged Colloids*, VCH Publishers, New York, 1996.
[137] P. Debye and E. Hückel, Zur Theorie der Elektrolyte, Physik. Zeitschr. **24**, 305–325 (1923).
[138] G.A. Parks, The isoelectric points of solid oxides, solid hydroxides and aqueous hydroxo complex systems, Chem. Rev. **65**, 177–198 (1977).
[139] R.J. Hunter, *Foundations of Colloid Science*, Vol. 1, Oxford University Press, Oxford, 1986.
[140] H.C. Hamaker, London-van der Waals attraction between spherical particles, Physica **4**, 1058–1072 (1937).
[141] W.C.K. Poon and P.B. Warren, Phase behaviour of hard-sphere mixtures, Europhys. Lett. **28**(7), 513–518 (1994).
[142] H. Sonntag and K. Strenge, *Coagulation Kinetics and Structure Formation*, VEB Deutscher Verlag der Wissenschaften, Kluwer Academic/Plenum, New York, 1988.
[143] J. Mahanty and B.W. Ninham, *Dispersion Forces*, Academic Press, New York, 1976.
[144] B.W. Ninham, K. Kurihara and O.I. Vinogradova, Hydrophobicity, specific ion adsorption and reactivity colloids, Surf. A: Physicochem. Eng. Aspects **123–124**, 7–12 (1997).
[145] B.W. Ninham and V. Yaminsky, Ion binding and ion specificity: the Hofmeister effect and Onsanger and Lifshitz theories, Langmuir **13**, 2097–2108 (1997).
[146] B.W. Ninham, On progress in forces since the DLVO theory, Adv. Colloid Interface Sci. **83**, 1–17 (1999).
[147] B.V. Derjaguin and L.D. Landau, Theory of the stability of strongly charged lyophobic sols and of the adhesion of strongly charged particles in solutions of electrolytes, Acta Physicochim. U.S.S.R. **14**, 633 (1941).
[148] E.J. Verwey and J.Th.G. Overbeek, *Theory of the Stability of Lyophobic Colloids*, Elsevier, Amsterdam, 1948.
[149] W.B. Russel, D.A. Saville and W.R. Schowalter, *Colloidal Dispersions*, Cambridge University Press, Cambridge, 1989.
[150] B.A. Pailthorpe and W.B. Russel, The retarded van der Waals interaction between spheres, J. Colloid Int. Sci. **89**(2), 563–566 (1982).
[151] T. Sugimoto, T. Takahashi, H. Itoh, S. Sato and A. Muramatsu, Direct measurement of interparticle forces by the optical trapping technique, Langmuir **13**(21), 5528–5530 (1997).
[152] S. Asakura and F. Oosawa, Interaction between particles suspended in solutions of macromolecules, J. Polym. Sci. **33**, 183 (1958).
[153] A. Vrij, Polymers at interfaces and the interactions in colloidal dispersions, Pure Appl. Chem. **48**, 471–483 (1976).
[154] S. Asakura and F. Oosawa, On interaction between two bodies immersed in a solution of macromolecules, J. Chem. Phys. **22**, 1255–1256 (1954).

[155] Y. Mao, M.E. Cates and H.N.W. Lekkerkerker, Depletion force in colloidal systems, Physica A **222**, 10–24 (1995).
[156] A. Einstein, On the movement of small particles suspended in stationary liquids required by the molecular-kinetic theory of heat (Über die von der molekularkinetischen Theorie der Wärme geforderte Bewegung von in ruhenden Flüssigkeiten suspendierten Teilchen), Annalen der Physik **17**, 123 (1905).
[157] H. de Hek and A. Vrij, Phase separation in non-aqueous dispersions containing polymer molecules and colloidal spheres, J. Colloid Interface Sci. **70**(3), 592–598 (1979).
[158] C. Pathmamanobaran, H. de Hek and A. Vrij, Phase seperation in mixtures of organophilic spherical silica particles and polymer molecules in good solvents, Colloid Polym. Sci. **259**, 769 (1981).
[159] S.M. Ilett, A. Orrock, W.C.K. Poon and P.N. Pusey, Phase behavior of a model colloid-polymer mixture, Phys. Rev. E **51**(2), 1344 (1995).
[160] O.D. Velev, A.M. Lenhoff and E.W. Kaler, A class of microstructured particles through colloidal crystallization, Nature (London) **287**, 2240 (2000).
[161] R.C. Salvarezza, L. Vázquez, H. Míguez, R. Mayoral, C. López and F. Meseguer, Edward-Wilkinson behavior of crystal surfaces grown by sedimentation of SiO_2 nanospheres, Phys. Rev. Lett. **77**(22), 4572–4575 (1996).
[162] M.O. Robbins, K. Kremer and G.S. Grest, Phase diagram and dynamics of Yukawa systems, J. Chem. Phys. **88**(5), 3286–3312 (1988).
[163] P.N. Pusey and W. van Megen, Phase behavior of concentrated suspensions of nearly hard colloidal spheres, Nature **320**, 340–342 (1986).
[164] M. Sullivan, K. Zhao, Ch. Harrison, R.H. Austin, M. Megens, A. Hollingsworth, W.B. Russel, Zhengdong Cheng, Th. Mason and P.M. Chaikin,Control of colloids with gravity, temperature, gradients, and electric fields, J. Phys.: Condens. Matter **15**, S11–S18 (2003).
[165] R. Tuinier, J. Rieger and C.G. de Kruif, Depletion-induced phase separation in colloid-polymer mixtures, Adv. Colloid Interface Sci. **103**, 1–31 (2003).
[166] N.M. Dixit and C.F. Zukoski, Kinetics of crystallization in hard-sphere colloidal suspensions, Phys. Rev. E **64**, 041604–041610 (2001).
[167] P. Pieranski, Colloidal crystals, Contemp. Phys. **24**(1), 25–73 (1983).
[168] I. Snook and W. van Megan, Calculation of the wave-vector dependent diffusion constant in concentrated electrostatically stabilized dispersions, J. Colloid Interface Sci. **100**(1), 194–202 (1984).
[169] A.P. Gast and W.B. Russel, Simple ordering in complex fluids, Phys. Today December, 24 (1998).
[170] N. Ise, How and why do like-charged particles in solution repel one another? Ordered regions in dilute solutions of macroions, Angew. Chem. Int. Ed. Engl. **98**(4), 323–334 (1986).
[171] S. Dosho, N. Ise, K. Ito, S. Iwai, H. Kitano, H. Matsuoka, H. Nakamura, H. Okumura, T. Ono, I.S. Sogami, Y. Ueno, H. Yoshida and T. Yoshiyama, Recent study of polymer latex dispersions, Langmuir **9**, 394–411 (1993).
[172] N.A. Clark, A.J. Hurd and B.J. Ackerson, Single colloid crystals, Nature **281**, 57–60 (1979).
[173] P. Pieranski, L. Strzelecki and B. Pansu, Thin colloidal crystals, Phys. Rev. Lett. **50**, 900 (1983).
[174] T. Okubo, Giant colloidal single crystals of polystyrene and silica spheres in deionized suspension, Langmuir **10**, 1695–1702 (1994).
[175] E.A. Kamenetzky, L.G. Magliocco and H.P. Panzer, Structure of solidified colloidal array laser filters studied by cryogenic transmission electron microscopy, Science **263**, 207–210 (1994).
[176] H.B. Sunkara, J.M. Jethmalani and W.T. Ford, Composite of colloidal crystals of silica in poly(methyl methacrylate), Chem. Mater. **6**, 362 (1994).
[177] M. Weissman, H.B. Sunkara, A.S. Tse and S.A. Asher, Thermally switchable periodicities from novel mesocopically ordered materials, Science **274**, 959–960 (1996).
[178] O. Vickreva, O. Kalinina and E. Kumacheva, Colloid crystal growth under oscillatory shear, Adv. Mater. **12**, 110–112 (2000).
[179] J. Zhu, M. Li, R. Rogers, W. Meyer and R.H. Ottewill, STS-73 space shuttle crew, W.Z.B. Russel and P.M. Chaikin, Crystallization of hard sphere colloids in μ-gravity, Nature **387**, 883 (1997).
[180] S. Beyer, Neue Wege zur Kristallisation von Nanopartikeln zu photonischen Kristallen, Diploma thesis, Paderborn, Germany, 2003.
[181] P. Richetti, J. Prost and P. Barois, Two-dimensional aggregation and crystallization of a colloidal suspension of latex spheres, J. Phys. Lett. **45**, L1137–L1143 (1984).
[182] S.-R. Yeh, M. Seul and B.I. Shraiman, Light-modulated electrokinetic assembly of planar colloidal arrays, Nature **386**, 57–59 (1997).

[183] Y. Solomentsev, M. Bohmer and J.L. Anderson, Electrophoretic cepositiion: a hydrodynamic model, Langmuir **13**, 6058 (1997).
[184] R.C. Hayward, D.A. Saville and I.A. Aksay, Electrophoretic assembly of colloidal crystals with optically tunable micropatterns, Nature **404**, 56–59 (2000).
[185] T. Gong and D.W.M. Marr, Electrically switchable colloidal ordering in confined geometries, Langmuir **17**, 2301–2304 (2001).
[186] C. Mio and D.W.M. Marr, Optical trapping for the manipulation of colloidal particles, Adv. Mater. **12**, 917–920 (2000).
[187] C. Mio and D.W.M. Marr, Tailored surfaces using optically manipulated colloidal particles, Langmuir **15**, 8565–8568 (1999).
[188] A. van Blaaderen, R. Ruel and P. Wiltzius, Template-directed colloidal crystallization, Nature (London) **385**, 321 (1997).
[189] K.E. Davis, W.B. Russel and W.J. Glantschnig, Settling suspensions of colloidal silica: observations and x-ray measurements, J. Chem. Soc. Faraday Trans. **87**, 411 (1991).
[190] P. Jiang, J.F. Bertone, K.S. Hwang and V.L. Colvin, Single-crystal colloidal multilayers of controlled thickness, Chem. Mater. **11**, 2132–2140 (1999).
[191] Y.C. Chan, M. Carles, Nikolaus J Sucher, M. Wong and Y. Zohar, Design and fabrication of an integrated microsystem for microcapillary electrophoresis, J. Micromech. Microeng. **13**, 914–921 (2003).
[192] H.A. Pohl, *Dielectrophoresis*, Cambridge University Press, Cambridge, 1978.
[193] T.B. Jones, *Electromechanics of Particles*, Cambridge University Press, Cambridge, 1995.
[194] S.O. Lumsdon, E.W. Kaler, J.P. Williams and O.D. Veleva, Dielectrophoretic assembly of oriented and switchable two-dimensional photonic crystals, Appl. Phys. Lett. **82**(6), 949–951 (2003).
[195] M. Golosovsky, Y. Saado and D. Davidov, Self-assembly of floating magnetic particles into ordered structures—a promising route for the fabrication of photonic bandgap materials, Appl. Phys. Lett. **75**, 4168–4170 (1999).
[196] N.D. Denkov, O.D. Velev, P.A. Kralchevsky, I.B. Ivanov, H. Yoshimura and K. Nagayama, Two-dimensional crystallization, Nature (London) **361**, 26 (1993).
[197] Q.H. Wei, D.M. Cupid and X.L. Xu, Controlled assembly of two-dimensional colloidal crystals, Appl. Phys. Lett. **77**, 1641–1643 (2000).
[198] G. Picard, Fine particle monolayers made by a mobile dynamic thin laminar flow (DTLF) device, Langmuir **14**(13), 3710–3715 (1998).
[199] N.D. Denkov, O.D. Velev, P.A. Kralchevsky, I.B. Ivanov, H. Yoshimura and K. Nagayama, Mechanism of formation of two-dimensional crystals from latex particles on substrates, Langmuir **8**, 3183–3190 (1992).
[200] A.S. Dimitrov and K. Nagayama, Continuous convective assembling of fine particles into morpho-colored two-dimensional arrays, Langmuir **12**, 1303–1311 (1996).
[201] O.D. Velev, N.D. Denkov, V.N. Paunov, P.A. Kralchevsky and K. Nagayama, Direct measurement of lateral capillary forces, Langmuir **9**, 3702 (1993).
[202] S. Rakers, L.F. Chi and H. Fuchs, Influence of the evaporation rate on the packing order of polydisperse latex monofilms, Langmuir **13**, 7121–7124 (1997).
[203] A.S. Dimitrov, T. Miwa and K. Nagayama, A comparison between the optical properties of amorphous and crystalline monolayers of silica particles, Langmuir **15**, 5257–5264 (1999).
[204] P.A. Kralchevsky, N.D. Denkov, V.N. Paunov, O.D. Velev, I.B. Ivanov, H. Yoshimura and K. Nagayama, Formation of two-dimensional colloid crystals in liquid films under the action of capillary forces, J. Phys.: Condens. Matter **6**, A395 (1994).
[205] R. Amos, J.G. Rarity, P.R. Tapster, T.J. Shepherd and S. Kitson, Fabrication of large-area face-centered-cubic hard-sphere colloidal crystals by shear alignment, Phys. Rev. E **61**, 2929 (2000).
[206] Yong-Hong Ye, F. LeBlanc, A. Hache and Vo-Van Truongb, Self-assembling three-dimensional colloidal photonic crystal structure with high crystalline quality, Appl. Phys. Lett. **78**(1), 52–54 (2001).
[207] D.H. Van Winkle and C.A. Murray, Layering transitions in colloidal crystals as observed by diffraction and direct lattice imaging, Phys. Rev. **34**, 562 (1986).
[208] S. Neser, C. Bechinger, P. Leiderer and T. Palberg, Finite size effects on the closest packing of hard spheres, Phys. Rev. Lett. **79**, 2348 (1997).
[209] S.H. Park, D. Qin and Y.X. Xia, Crystallization of meso-scale particles over large areas, Adv. Mater. **10**, 1028–1031 (1998).
[210] S.H. Park and Y. Xia, Crystallization of meso-scale particles over large areas and its application in fabricating tunable optical filters, Langmuir **15**, 266–273 (1999).

[211] B. Gates, D. Qin and Y. Xia, Assembly of nanoparticles into opaline structures over large areas, Adv. Mater. **11**, 466–469 (1999).
[212] Y. Lu, Y. Yin and Y. Xia, A self-assembly approach to the fabrication of patterned 2D arrays of microlenses of organic polymers, Adv. Mater. **13**, 34–37 (2001).
[213] K. Lin, J.C. Crocker, V. Prasad, A. Schofield, D.A. Weitz, T.C. Lubensky and A.G. Yodh, Entropically driven colloidal crystallization on patterned surfaces, Phys. Rev. Lett. **85**, 1770 (2000).
[214] Y.-H. Ye, S. Badilescu, Vo-Van Truong, P. Rochon and A. Natansohn, Self-assembly of colloidal spheres on patterned substrates, Appl. Phys. Lett. **79**, 872–874 (2001).
[215] Y. Yin, Y. Lu and Y. Xia, A self-assembly approach to the formation of asymmetric dimers from monodispersed spherical colloids, J. Am. Chem. Soc. **123**, 771–772 (2001).
[216] Y. Yin and Y. Xia, Self-assembly of monodispersed col1oidal spheres into complex aggregates with well-defined sizes, shapes, and structures, Adv. Mater. **13**, 267–271 (2001).
[217] Y. Yin, Y. Lu and Y. Xia, Self-assembly of monodispersed spherical colloids into 1D chains with well-defined lengths and structures, J. Mater. Chem. **11**, 987–989 (2001).
[218] E. Kim, Y. Xia and G.M. Whitesides, Two- and three-dimensional crystallization of polymeric microspheres by micromolding in capillaries, Adv. Mater. **8**, 245–247 (1996).
[219] S.M. Yang and G.A. Ozin, Opal-chips: vectorial growth of colloidal crystal patterns inside silicon wafers, Chem. Commun. 2507–2508 (2000).
[220] G.A. Ozin and M.Y. Yang, Race for the photonic chip, opal-patterned chips, Adv. Funct. Mater. **11**, 1–10 (2001).
[221] Y. Lu, Y. Yin and Y. Xia, Three-dimensional photonic crystals with non-spherical colloids as building blocks, Adv. Mater. **13**(6), 415 (2001).
[222] J. Tien, A. Terfort and G.M. Whitesides, Microfabrication through electrostatic self-assembly, Langmuir **13**, 5349–5355 (1997).
[223] K.M. Chen, X. Jiang, L.C. Kimerling and P.T. Hammond, Selective self organization of colloids on patterned polyelectrolyte templates, Langmuir **26**, 7825–7834 (2000).
[224] B.T. Holland, C.F. Blanford, T. Do and A. Stein, Synthesis of highly ordered three-dimensional macroporous structures of amorphous or crystalline inorganic oxides, phosphates and hybrid composites, Chem. Mater. **11**, 795–805 (1999).
[225] M. Deutsch, Y.A. Vlasov and D.J. Norris, Conjugated-polymer photonic crystals, Adv. Mater. **12**, 1176 (2000).
[226] A. von Rhein, Synthese, Dotierung und Analyse von TiO_2-Nanopartikeln für die Photonik, Diploma thesis, Paderborn, Germany, 2003.
[227] J.S. Yin and Z.L. Wang, Template-assisted self-assembling and cobalt doping of ordered meroporous titania nanostructures, Adv. Mater. **11**, 469 (1999).
[228] Y.A. Vlasov, N. Yao and D.J. Norris, Synthesis of photonic crystals for optical wavelengths from semiconductor quantum dots, Adv. Mater. **11**, 165 (1999).
[229] V.N. Subramanian, J.D. Manoharan, D.J. Thorne, and D. Pine, Ordered macroporous materials by colloidal assembly: a possible route to photonic bandgap materials, Adv. Mater.**11**, 1261–1265 (1999).
[230] A.A. Zakhidov, R.H. Baughman, Z. Iqbal, C. Cui, I. Khayrullin, S.O. Dantas, J. Marti and V.G. Ralchenko, Carbon structures with three-dimensional periodicity at optical wavelengths, Science **282**, 897–901 (1998).
[231] A. Blanco, E. Chomski, S. Grabtchak, M. Ibisate, S. John, S.W. Leonard, C. López, F. Meseguer, H. Míguez, J.P. Mondía, G.A. Ozin, O. Toader and H.M. van Driel, Large-scale synthesis of a silicon photonic crystal with a complete three-dimensional bandgap near 1.5 micrometers, Nature **405**, 437–440 (2000).
[232] H. Miguez, E. Chomski, F. Garcia-Santamaria, M. Ibisate, S. John, C. Lopez, F. Meseguer, J.P. Mondia, G.A. Ozin, O. Toader and H.M. van Driel, Photonic bandgap engineering in germanium inverse opals by chemical vapor deposition, Adv. Mater. **13**, 1634–1637 (2001).
[233] C.C. Cheng, A. Scherer, V. Arbet-Engels and E. Yablonovitch, Lithographic band gap tuning in photonic band gap crystals, J. Vac. Sci. Technol. B**14**, 4110–4114 (1996).
[234] C.A. Murray and D.G. Grier, Colloidal crystals, Am. Sci. **83**, 238 (1995).
[235] D.G. Grier (Ed.), *From Dynamics to Devices: Directed Self-Assembly of Colloidal Materials*, a special issue in *MRS Bull*. **23**(10), 21 (1998).
[236] D.H. Everett, *Basic Principles of Colloid Science*, Royal Society of Chemistry, London, 1988.
[237] R.J. Hunter, *Introduction to Modern Colloid Science*, Oxford University Press, Oxford, 1993.

[238] Y. Xia, B. Gates, Y. Yin and Y. Lu, Monodispersed colloidal spheres: old materials with new applications, Adv. Mater. **12**, 693–713 (2000).
[239] E. Matijevic, Uniform inorganic colloid dispersions: achievements and challenges, Langmuir **10**, 8 (1994).
[240] E. Matijestic (Ed.), *Fine Particles*, a special issue in *MRS Bulletin* **14**(12), 18 (1989).
[241] R.K. Iler, *The Chemistry of Silica*, Wiley-Interscience, New York, 1979.
[242] I. Piirma (Ed.), *Emulsion Polymerization*, Academic Press, New York, 1982.
[243] G.W. Poehlein, R.H. Ottewill and J.W. Goodwin (Eds.), *Science and Technology of Polymer Colloids*, Vols. 1 and 2, Proc. of ASI, Bristol, England, 1983.
[244] A.D. Dinsmore, J.C. Crocker and A.G. Yodh, Self-assembly of colloidal crystals, Curr. Opin. Colloid Interface **3**, 5–11 (1998).
[245] J.H. Holtz and S.A. Asher, Polymerized colloidal crystal hydrogel films as intelligent chemical sensing materials, Nature **389**, 829–832 (1997).
[246] R. Mayoral, J. Requena, C. López, S.J. Moya, H. Míguez, L. Vázquez, F. Meseguer, M. Holgado, A. Cintas and A. Blanco, 3D long range ordering of submicrometric SiO_2 sintered superstructures, Adv. Mater. **9**, 257–260 (1997).
[247] I.I. Tarhan and G.H. Watson, Photonic band structure of fcc colloidal crystals, Phys. Rev. Lett. **76**, 315 (1996).
[248] J.D. Joannopoulos, R.D. Meade and J.N. Winn, *Photonic Crystals: Molding the Flow of Light*, Princeton University Press, Princeton, 1995.
[249] J.T. Londergan, J.P. Carini and D.P. Murdock, *Binding and Scattering in Two-Dimensional Systems: Application to Quantum Wires, Waveguides and Photonic Crystals*, Springer, Berlin, 1999.
[250] Photonic crystals and light localization, in *Photonic Crystals and Light Localization in the 21st Century 2001, Proceedings of a NATO Advanced Study Institute*, Crete, Greece, Ed C. Soukoulis, NATO Science Series, Kluwer, Dodrecht, 2000.
[251] K. Sakoda, *Optical Properties of Photonic Crystals*, Springer, Berlin, 2001.
[252] S.G. Johnson and J.D. Joannoupolos, *Photonic Crystals: The Road from Theory to Practice*, Kluwer, Boston, 2002.
[253] W.J. Parak, D. Gerion, T. Pellegrino, D. Zanchet, C. Micheel, S.C. Williams, R. Boudreau, M.A. Le Gros, C.A. Larabell and A.P. Alivisatos, Biological applications of colloidal nanocrystals, Nanotechnology **14**, R15–R27 (2003).
[254] T.A. Taton, Boning up on biology, Nature **412**, 491–492 (2001).
[255] W.C.W. Chan and S. Nie, Quantum-dot bioconjugates for ultrasensitive nonisotopic detection, Science **281**, 2016–2018 (1998).
[256] S. Pathak, S.-K. Choi, N. Arnheim and M.E. Thompson, Hydroxylated quantum dots as luminescent probes for in situ hybridization, J. Am. Chem. Soc. **123**(17), 4103–4104 (2001).
[257] E. Klarreich, Biologists join the dots, Nature **413**, 450–452 (2001).
[258] P.S. Weiss, Nanotechnology: molecules join the assembly line, Nature **413**, 585–586 (2001).
[259] S.J. Rosenthal, I. Tomlinson, E.M. Adkins, S. Schroeter, S. Adams, L. Swafford, J. McBride, Y. Wang, L.J. DeFelice and R.D. Blakely, J. Am. Chem. Soc.**124**, 4586–4594 (2002).
[260] J.K. Jaiswal, H. Mattoussi, J.M. Mauro and S.M. Simon, Long-term multiple color imaging of live cells using quantum dot bioconjugates, Nat. Biotechnol. **21**, 47–51 (2003).
[261] B. Dubertret, P. Skourides, D.J. Norris, V. Noireaux, A.H. Brivanlou and A. Libchaber, An in vivo imaging of quantum dots encapsulated in phospholipid micelles, Science **298**, 1759–1762 (2002).
[262] M.E. Akerman, W.C.W. Chan, P. Laakkonen, S.N. Bhatia and E. Ruoslahti, Nanocrystal targeting in vivo, Proc. Natl Acad. Sci. USA **99**, 12617–12621 (2002).
[263] M.X. Wu, H. Liu, J. Liu, K.N. Haley, J.A. Treadway, J.P. Larson, N. Ge, F. Peale and M.P. Bruchez, Immunofluorescent labeling of cancer marker Her2 and other cellular targets with semiconductor quantum dots, Nat. Biotechnol. **21**, 41–46 (2003).
[264] M. Han, X. Gao, J.Z. Su and S. Nie, Quantum-dot-tagged microbeads for multiplexed optical coding of biomolecules, Nat. Biotechnol. **19**, 631–635 (2001).
[265] S.J. Rosenthal, Bar-coding biomolecules with fluorescent nanocrystals, Nat. Biotechnol. **19**, 621–622 (2001).
[266] A.P. Alivisatos, Less is more in medicine—sophisticated forms of nanotechnology will find some of their first real-world applications in biomedical research, disease diagnosis and, possibly, therapy, Sci. Am. **285**, 66–73 (2001).

[267] S. Sun, C.B. Murray, D. Weller, L. Folks and A. Moser, Monodisperse FePt nanoparticles and ferromagnetic nanocrystal superlattices, Science **287**, 1989–1992 (2000).
[268] S. Onodera, H. Kondo and T. Kawana, Materials for magnetic-tape media, MRS Bull. **21**(9), 35 (1996).
[269] K. O'Grady, R.L. White and P.J. Grundy, Whither magnetic recording, J. Magn. Magn. Mater. **177–181**, 886891 (1998).
[270] R.L. White, R.M.H. New and R.F.W. Pease, Patterned media: a viable route to 50 Gbit/in^2 and up for magnetic recording, IEEE Trans. Magn. **33**, 990–995 (1997).
[271] G. Ennas, A. Mei, A. Musinu, G. Piccaluga, G. Pinna and S. Solinas, Sol-gel preparation and characterization of Ni-SiO^2 nanocomposites, J. Non-Cryst. Solids **232–234**, 587 (1998).
[272] G.H. Wang and A. Harrison, Preparation of iron particles coated with silica, J. Colloid Interface Sci. **217**, 203–207 (1999).
[273] M. Ohmori and E. Matijevic, Preparation and properties of uniform coated inorganic colloidal particles: 8. Silica on iron, J. Colloid Interface Sci. **160**, 288 (1993).
[274] S. Hui, Y.D. Zhang, T.D. Xiao, M. Wu, S. Ge, W.A. Hines, J.I. Budnick, M.J. Yacaman and H.E. Troiani, in *Nanophase and Nanocomposite Materials IV*, *Mater. Res. Soc. Symposium Proceedings*, Warrendale, PA, Vol. 703, Ed. S. Komarneni, R.A. Vaia, G.Q. Lu, J.-I. Matsushita and J.C. Parker, Material Research Society, Warrendale, PA, 2002.
[275] A.P. Philipse, M.P.B.V. Bruggen and C. Pathmamanoharan, Magnetic silica dispersions: preparationand stability of surface-modified silica particles with a magnetic core, Langmuir **10**, 92 (1994).
[276] G.-M. Chow and K.E. Gonsalves (Eds.), *Nanotechnology Molecularly Designed Materials*, American Chemical Society, Washington, DC, 1996, p. 42.
[277] Q. Liu, Z. Xu, J.A. Finch and R. Egerton, A novel two-step silica coating process for engineering magnetic nanocomposites, Chem. Mater. **10**(12), 3936–3940 (1998).
[278] H.W. Deckman and J.H. Dunsmuir, Natural lithography, Appl. Phys. Lett. **41**, 377–379 (1982).
[279] C. Hulteen and R.P. Van Duyne, Nanosphere lithography: a materials general fabrication process for periodic particle array surfaces, J. Vac. Sci. Technol. A **13**, 1553–1558 (1995).
[280] F. Burmeister, C. Schäfle, B. Keilhofer, C. Bechinger, J. Boneberg and P. Leiderer, From mesoscopic to nanoscopic surface structures: lithography with colloid monolayers, Chem. Eng. Technol. **21**, 761 (1998).
[281] F. Burmeister, W. Badowsky, T. Braun, S. Wieprich, J. Boneberg and P. Leiderer, Colloid monolayer lithography—a flexible approach for nanostructuring of surfaces, Appl. Surface Sci. **144–145**, 461 (1999).
[282] H. Fang, R. Zeller and P.J. Stiles, Appl. Phys. Lett. **55**, 1433 (1989).
[283] T. Iwabuchi, C. Chuang, G. Khitrova, M.E. Warren, A. Chavez-Pirson, H.M. Gibbs, D. Sarid and M. Gallagher, Fabrication of GaAs nanometer scale structures by dry etching, Proc. SPIE **1284**, 142 (1990).
[284] M. Green, M. Garcia-Parajo and F. Khaleque, Quantum pillar structures on n^+gallium arsenide fabricated using "natural" lithography, Appl. Phys. Lett. **62**, 264–266 (1993).
[285] W.D. Dozier, K.P. Daly, R. Hu, C.E. Platt and M.S. Wire, Fabrication of high-T_c Josephson effect devices by natural lithography, IEEE Trans. Magn. **27**(2), 3223–3226 (1991).
[286] R.F. Cregan, B.J. Mangan, J.C. Knight, T.A. Birks, P.S. Russell, P.J. Roberts and D.C. Allan, Single-mode photonic band gap guidance of light in air, Science **285**, 1537–1539 (1999).
[287] P.S.J. Russell, T.A. Birks, J.C. Knight, R.F. Cregan, B. Mangan and J.P. De Sandro, Silica/air photonic crystal fibres, Japan. J. Appl. Phys., Part 1 **37**, 45–48 (1998)
[288] A. Guinier and G. Fournet, *Small-Angle Scattering of X-rays*, Wiley, New York, 1955.
[289] G. Subramania, K. Constant, R. Biswas, M.M. Sigalas and K.M. Ho, Optical photonic crystals fabricated from colloidal systems, Appl. Phys. Lett. **74**, 3933 (1999).
[290] L. Bechger, A.F. Koenderink and W.L. Vos, Emission spectra and lifetimes of R6G dye on silica-coated titania powder, Langmuir **18**(6),2444–2447 (2002).